NASA CR-135364

NIOBIUM-GERMANIUM SUPERCONDUCTING TAPES FOR HIGH-FIELD MAGNET APPLICATIONS

A. I. Braginski, G. W. Roland, M. R. Daniel
and J. A. Woollam

WESTINGHOUSE RESEARCH AND DEVELOPMENT CENTER

prepared for

NATIONAL AERONAUTICS AND SPACE ADMINISTRATION

NASA Lewis Research Center

Contract NAS3-20233

1. Report No.	2. Government Accession No.	3. Recipient's Catalog No.
CR-135364		

4. Title and Subtitle	5. Report Date
NIOBIUM-GERMANIUM SUPERCONDUCTING TAPES FOR HIGH-FIELD MAGNET APPLICATIONS	November 1977
	6. Performing Organization Code
7. Author(s)	8. Performing Organization Report No.
A. I. Braginski, G. W. Roland, M. R. Daniel, and J. A. Woollam	77-9F1-HYSUC-R9
	10. Work Unit No.
9. Performing Organization Name and Address	11. Contract or Grant No.
Westinghouse Electric Corporation Research and Development Center 1310 Beulah Road Pittsburgh, Pennsylvania 15235	NAS3-20233
	13. Type of Report and Period Covered
12. Sponsoring Agency Name and Address	Contractor Report (Final) 04-19-1976 to 11-19-1977
National Aeronautics and Space Administration Washington, DC 20546	14. Sponsoring Agency Code

15. Supplementary Notes

Project Manager, John A. Woollam, Cryophysics Section, Physical Science Division, NASA-Lewis Research Center, Cleveland, Ohio 44135

16. Abstract

A process of fabricating superconducting Nb_3Ge tapes by chemical vapor deposition (CVD) has been developed and tapes up to 10 meters long fabricated. The typical properties achieved were: critical temperature T_c = 20 K, upper critical field H_{c2} = 29 tesla at 4.2 K and J_c = 3 to 4 x 10^8 A m^{-2} at 4.2 K, 18 tesla. The best J_c achieved in these conditions was $\sim 10^9$ A m^{-2}. The relative depression of T_c and H_{c2} compared with the best thin film samples sputtered on sapphire was due to the presence of Nb_5Ge_3 second-phase particles used as flux pinning centers and to strains induced by thermal mismatch with Hastelloy B tape substrates. A peculiar field dependence of flux pinning force that was observed in both CVD and sputtered Nb_3Ge indicated a premature pin-breaking mechanism or a phase inhomogeneity. Directions of further optimization work were defined.

17. Key Words (Suggested by Author(s))	18. Distribution Statement
Superconductivity, conductor, tape, high, field, magnet, niobium, germanium	Unclassified -- unlimited

19. Security Classif. (of this report)	20. Security Classif. (of this page)	21. No. of Pages	22. Price*
Unclassified	Unclassified	103	

* For sale by the National Technical Information Service, Springfield, Virginia 22161

CONTENTS

LIST OF FIGURES

LIST OF TABLES

"Page missing from available version"

SUMMARY

Nb_3Ge superconducting tape conductor fabricated by chemical vapor deposition (CVD) can make it possible to construct very high-field *superconducting magnets capable of attaining 20 to 25 tesla at 4.2 Kelvin.* The objective of this NASA program was to investigate and optimize the high-field properties of Nb_3Ge tape samples in view of their future application in scientific laboratory magnets and nuclear fusion magnets.

A process of fabricating superconducting Nb_3Ge tapes by CVD has been developed and tapes up to 10 meters long fabricated. The typical properties achieved were: critical temperature T_c = 20 K, upper critical field H_{c2} = 29 tesla at 4.2 K and J_c = 3 to 4 x 10^8 A m^{-2} at 4.2 K, 18 tesla. The best J_c achieved in these conditions was $\sim 10^9$ A m^{-2}. The relative depression of T_c and H_{c2} compared with the best thin film samples sputtered on sapphire ($T_c \simeq$ 22 to 23 K, H_{c2} = 36 to 38 tesla at 4.2 K) was due to the presence of Nb_5Ge_3 second-phase particles used as flux pinning centers and to strains induced by thermal mismatch with Hastelloy B tape substrates. A peculiar field dependence of flux pinning force that was observed in both CVD and sputtered Nb_3Ge indicates a premature pin-breaking mechanism or a phase inhomogeneity. Further optimization work should concentrate on elucidating the problem of premature pin breaking vs phase inhomogeneity, preparing multilayerd single-phase Nb_3Ge films, testing of mechanical properties of Nb_3Ge and developing long, composite Nb_3Ge conductors. Eventually, test solenoids and prototype magnets should be constructed.

"Page missing from available version"

NIOBIUM-GERMANIUM SUPERCONDUCTING TAPES FOR HIGH-FIELD MAGNET APPLICATIONS

A. I. Braginski, G. W. Roland, M. R. Daniel

Westinghouse R&D Center
Pittsburgh, Pennsylvania 15235

and J. A. Woollam

NASA-Lewis Research Center
Cleveland, Ohio 44135

ABSTRACT

A process of fabricating superconducting Nb_3Ge tapes by chemical vapor deposition (CVD) has been developed and tapes up to 10 meters long fabricated. The typical properties achieved were: critical temperature T_c = 20 K, upper critical field H_{c2} = 29 tesla at 4.2 K and J_c = 3 to 4 x 10^8 A m^{-2} at 4.2 K, 18 tesla. The best J_c achieved in these conditions was $\sim 10^9$ A m^{-2}. The relative depression of T_c and H_{c2} compared with the best thin film samples sputtered on sapphire was due to the presence of Nb_5Ge_3 second-phase particles used as flux pinning centers and to strains induced by thermal mismatch with Hastelloy B tape substrates. A peculiar field dependence of flux pinning force that was observed in both CVD and sputtered Nb_3Ge indicated a premature pin-breaking mechanism or a phase inhomogeneity. Directions of further optimization work were defined.

1. INTRODUCTION

The overall objective of this program was to develop and characterize Nb_3Ge* superconducting tape for application in superconducting magnets capable of generating very high fields, up to 20 tesla or even above.

Gavaler discovered in 1973 that Nb_3Ge can have a high critical temperature, T_c, in excess of 22 K when prepared by low energy dc sputtering technique.[1] In 1974 T_c onsets of 23 K were reached and it was also found that the material has a very high upper critical field, H_{c2} = 36 to 38 tesla at 4.2 K.[2] For a thin sputtered sample of Nb_3Ge the critical current density was $J_c \simeq 1 \times 10^9$ A m^{-2} at 21 tesla, 4.2 K.[2] Hence, it became clear that the material will be useful for very high field applications provided that a practical conductor could be formed in a viable large-scale process. Indeed, it was shown in 1974 to 1975 that Nb_3Ge can be grown by chemical vapor deposition (CVD), which lends itself readily to the manufacture of lengths of conductor in tape form.[3,4] The Westinghouse study of CVD Nb_3Ge was at that stage supported in part by the Air Force Office of Scientific Research.

The development of Nb_3Ge tape conductor at Westinghouse was initially (1975 to 1976) sponsored by the U. S. Energy Research and Development Administration with the aim to evaluate a possible low-field application in superconducting transmission lines [Contract No. E(11-1)-2522]. That program was substantial in size and laid solid ground for the preparation of Nb_3Ge by CVD. Its end results are reported in references 5 to 7. In 1976 the present program was instituted to optimize the

---

* The formula Nb_3Ge is used as a generic term for the high-critical temperature, superconducting A15 phase. Its actual composition may deviate from ideal A_3B.

Nb_3Ge tapes for high-field magnet application by building upon the results obtained in the above ERDA program. The original goals and tasks of the present program are given in the Statement of Work (Appendix I). Subsequently, due to progress in the ERDA study, the scope of this work was extended to include the effect of dopants upon the high-field properties of Nb_3Ge. It was also agreed between the NASA Project Manager and Westinghouse that the quoted above properties of thin sputtered films will serve as a target for the study, and that tapes longer than the originally planned 0.3 meter will be fabricated.

In the course of this work established were the effects of deposition temperature upon H_{c2} and the high-field J_c (up to 17.5 T, 4.2 K) as well as the effects of several dopants: Nb_5Ge_3, NbN and NbC. Lengths of tapes up to 10 meters have been fabricated and evaluated. Tape specimens were delivered to NASA. The target properties of Nb_3Ge were approached although not attained in full. Directions for further work aimed at attaining and exceeding the target properties were formulated.

In conclusion, this program has demonstrated long Nb_3Ge tape conductors capable of performing adequately up to 18 tesla at 4.2 K. The program has also identified problems to be solved for a further high-field performance improvement.

2. THE CVD PROCESS AND REACTOR SYSTEM

2.1 Background

The chemical vapor deposition of Nb-Ge layers occurs at elevated temperatures by hydrogen reduction of a niobium and germanium chloride vapor mixture. General information about the Westinghouse process development is available in the literature[8-9] so that there is no need to reproduce it here. However, for the convenience of the reader, Appendix II contains a revised excerpt from Reference 5 describing the process and the moving tape CVD reactor which evolved from the ERDA's program. Appendix II describes the status at the end of that program (June 1976) and also gives the definition of process parameters used in the present report.

After June 1976 further changes and improvements in CVD of Nb_3Ge resulted from the work done under this program. Changed or modified were:

1. chloride vapor species.
2. the CVD reactor
3. some process parameters.

Below is given a brief description of major modifications.

2.2 Chlorides

In the moving tape CVD reactor the deposition zone must be short to preserve uniformity of the deposit in spite of the existence of a composition profile such as that discussed in Appendix II. However, shorter zone results in a reduced growth rate at any tape speed. As discussed in Section 2.4 the zone length was set at 10 cm only. Accordingly, maintaining a realistic growth rate became critical and material losses in

the mixer zone had to be eliminated. Hence, $NbCl_5$ and $GeCl_4$ were introduced. These chlorides are stable at relatively low mixing temperatures and have higher vapor pressure than $NbCl_4$ and $GeCl_2$.

Chlorination of the Nb bed to form $NbCl_5$ has been performed at 250 to 280°C by injecting a mixture of 10 vol. % Cl_2 (UHP grade, Matheson Company) and Ar (99.985%, Burdox). It was shown by Newkirk at Los Alamos Scientific Laboratory (LASL) that at relatively low temperatures $NbCl_5$ is produced as the only species if maintained at a low partial pressure. In the present case it was verified by collecting the vapor condensate that the reaction indeed produced $NbCl_5$. The quantitative character of the reaction (i.e., that it goes to completion) was verified by determining the Nb weight loss resulting from chlorination. Table 1 shows that for 10 cases out of 12 Nb consumption was within 2% of theoretical when chlorinating at a standard Cl_2 flow rate of 100 cm^3/min with manual flow control. Good reproducibility was achieved as long as the Nb bed temperature was maintained in the above-given temperature range. Since in the reactor system the hydrogen was preheated by flowing around the Nb and Ge beds, a 30 min. equilibrium time was needed after introducing the hydrogen. Temperature changes caused by the heat of the chlorination reaction were within acceptable limits.

At a double chlorination rate in runs 432 and 444 the Nb consumption was 96 and 95% respectively which was still acceptable. No significant effect of the bed depletion was observed after the 345 min. long run 444 (in that run an $\sim$ 10m long tape was deposited with 3 to 5 μm of Nb-Ge on each side of the substrate).

Chlorination of the Ge bed to form $GeCl_4$ was performed between 210 and 310°C with no strong dependence upon the temperature as shown in Table 1. Satisfactory control of the reaction rate was achieved after substituting for Cl_2 a 10% Cl_2-Ar mixture to improve the gas flow control. Chlorine flow rates in the typical range of 20 to 25 cm^3/min could not be controlled reliably without electronic mass flow controllers.* However,

*After three years of use the mass flow meters used for electronic control deteriorated and were disconnected during the program.

Table 1

Niobium and Germanium Chlorination to $NbCl_5$ and $GeCl_4$.
Results Expressed as Percent of Nb and Ge Weight Loss
Calculated for the Reaction. Thirteen Consecutive Runs.
Temperature of Nb: 250 to 270°C.

Run Number	Run Time Minutes	Nb Weight Loss %	Ge Weight Loss %	Ge Bed Temperature	Comment
430	282	100.9	100.0*	245 ± 5	
431	178	99.2	98.3*	238 ± 2	
432	100	96.0	109.9*	237 - 251	double Cl_2 rate - 200 cm^3/min.
433	--	--	--	230 ± 2	run aborted
434	156	100.0	101.6*	244 ± 2	
435	396	100.1	99.1	213 - 227	
436	124	102.4	102.2*	230 ± 5	
437	274	100.2	98.8*	309 ± 5	
438	239	101.3	--	299 ± 3	"epitaxial" run
439	383	96.5	100.8*	312 ± 2	
440	390	100.4	99.2	307 ± 1	
441	367	100.0	100.4	306 ± 1	
442	381	100.0	98.3*	305 ± 2	
Average	--	100.4	100.2		double rate run not included

*Chlorination rate was changed several times during the run to change the ratio $\frac{Nb}{Ge}$ = s.

the manual flow rate control in the range of 200 to 250 cm^3/min typical for the 10% mixture was found adequate as illustrated by Table 1.

After introducing the above modifications the loss of material in the mixer zone that was kept at 380 to 400°C was practically eliminated: the mixer weight increase was of the order of 1 gram or less in a typical run lasting several hours. Prior pick-up rate (Appendix II) was 7 to 8 grams per hour.

As a result of the change described above the deposition conditions were somewhat altered. At the deposition temperatures $NbCl_4$ and $GeCl_2$ are the stable species. When introducing $NbCl_5$ and $GeCl_4$ the excess chlorine dissociates and is present in the reaction atmosphere in addition to the other vapor components. This could have reduced the process efficiency but did not significantly affect the growth rate.

2.3 CVD Reactor

The following major modifications of the reactor described in Appendix II were introduced:

1. The gas flow path between the mixer and the deposition zone was shortened from ∿ 40 cm to ∿ 5 cm as shown in Figure 1. This cut down the material losses along that path very significantly and increased the growth rate by ∿ 50%. The position of the masking track MT1 (Figure 1) was chosen based on the X-ray analysis of the deposit profile.

2. The use of a short deposition zone (between MT1 and and MT2, Figure 1) permitted the elimination of the long Marshall furnace seen in Figure 8, Appendix II. The deposition now occurred in the cross furnace previously used for gas preheating only. The cross furnace was on both ends buffered by 10 cm long end furnaces. The modified reactor is shown in Figure 2. To improve the temperature uniformity

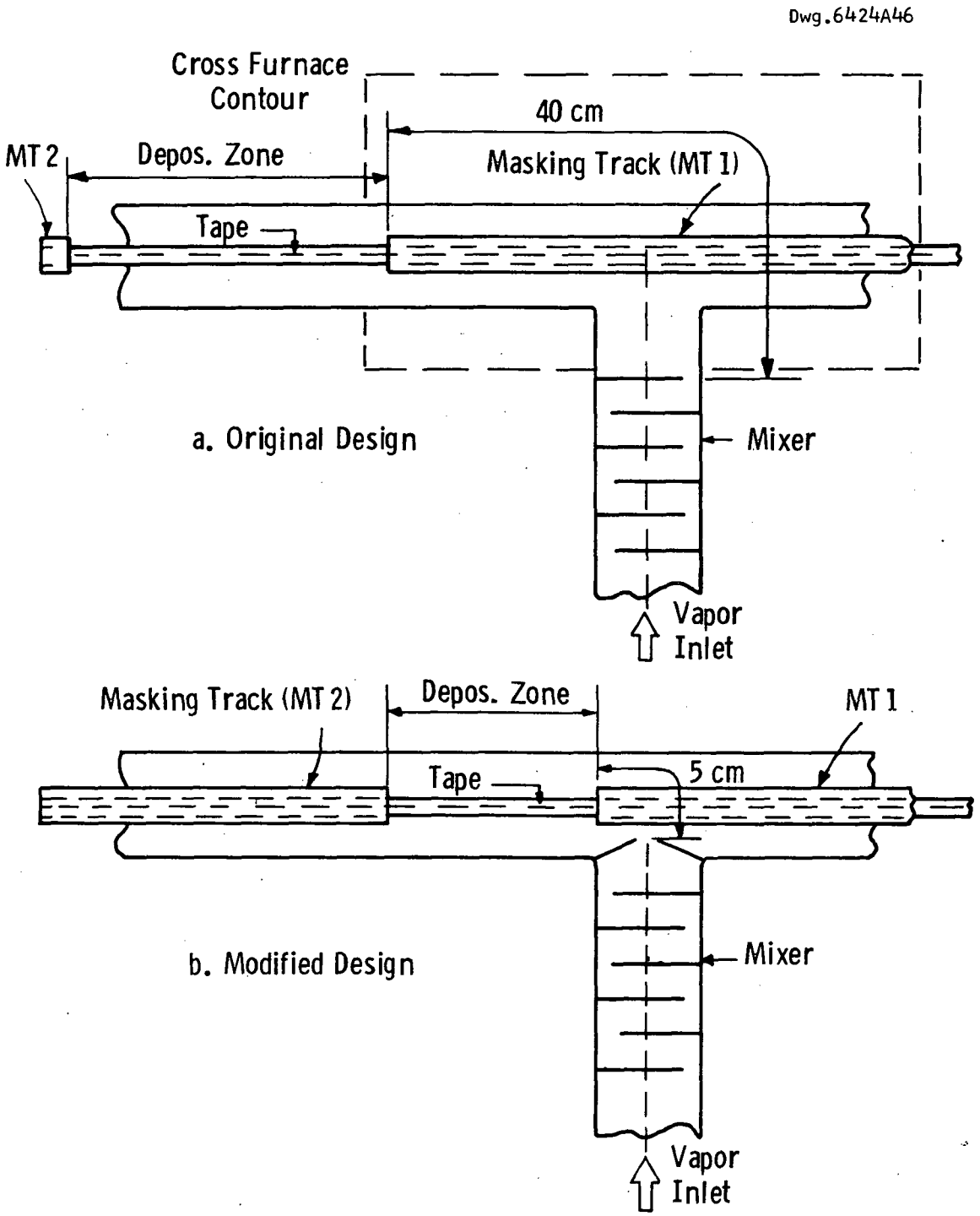

Fig. 1—The CVD reactor geometry

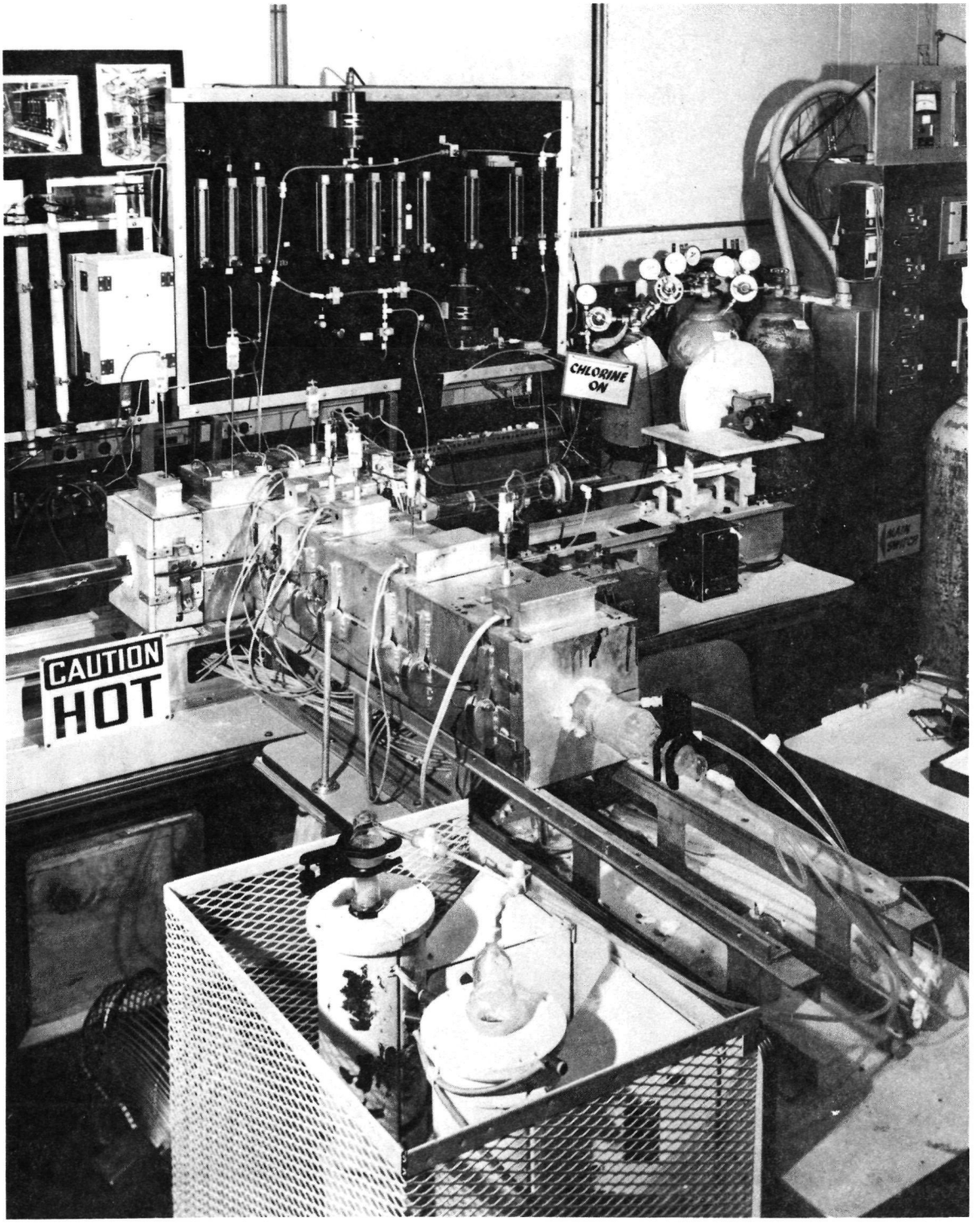

Figure 6 — The CVD reactor for continuous tape and wire/fiber coating with Nb_3Ge.

along the cross furnace a 1015 steel liner was implemented. The liner was 40 cm long. Its wall thickness was 0.16 cm. Cross furnace heaters were modified to obtain a steep temperature ramp between the mixer and the tape track MT1 and to minimize the temperature dip along the tape unavoidably resulting from the injection of Ar + H_2 + chloride vapor mixture having a temperature of $\sim$ 400°C. The final temperature profile along the major axis of the ractors is shown in Figure 3 for the typical deposition temperature, T_d = 850°C. The temperature increment along the 10 cm deposition zone was an acceptable +10°C.

3. The fused-silica masking tracks having a circular section $\sim$ 1 cm in diameter (MT in Figure 1) were eventually replaced with flattened 1015 steel tracks 9 mm wide, with 0.25 mm wall thickness and 0.25 to 0.50 mm clearance. The circular profile of silica tracks, particularly MT1, produced a "shadow" in the deposition zone resulting in a very nonuniform distribution of deposit on the tape. The 1015 steel tracks were geometrically similar to the original stainless steel masking tracks eliminated because of the deposit contamination (Appendix II). The use of soft steel such as 1015 minimized the contamination problem (this observation was originally made by Newkirk at LASL). Auger and secondary ion mass spectroscopy (SIMS) analyses indicated no presence of iron in the bulk of the deposit. The SIMS sensitivity limit in this case was better than 10 ppm. However, due to the tape contact with the mask at high temperature an iron-containing diffusion layer formed near the

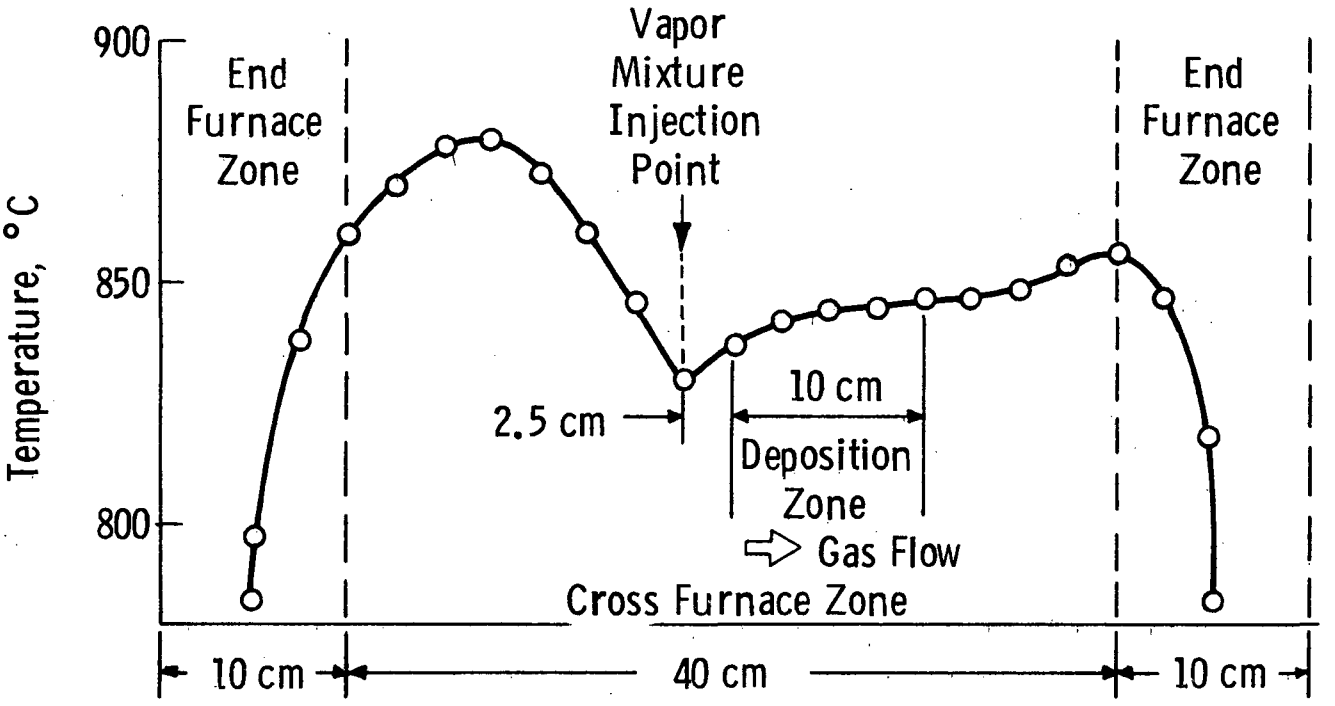

Fig. 3—Temperature profile along the major axis ot the CVD reactor; nominal temperature: $T_d = 850°C$

tape surface. The thickness of this layer was of the order of 1000 Å.

4. The substrate ohmic heating by electric current (Appendix II) was extensively tested and eventually abandoned. There were two main reasons for this decision:

   (a) Although the external resistive furnace was kept at a low temperature of 500 to 600°C, deposition on tube walls occurred due to radiation heating by the tape substrate. Lower external furnace temperatures were not practical because of excessive power density in the tape resulting in local overheating and "hot spot" formation. With the furnace kept at ∿ 500°C the gas phase depletion along the deposition zone has not been reduced significantly, and the rate of Nb-Ge deposition on the tape was not increased markedly over what was typical for the standard resistive furnace heating. A different reactor design eliminating the thermally insulating furnaces around the tube and using radiation reflective tube walls would have been necessary to benefit from the direct substrate heating. Such drastic change was beyond the scope of this program.

   (b) The Hastelloy B substrate tape, 25 μm thick, has experienced significant plastic flow under tension when heated by current. Constant tension must be applied to the tape for proper positioning along the major axis of the deposition tube. A calibrated, adjustable spring system has been used to

apply the tension. In the absence of electric current forces up to 1000 grams did not produce significant tape deformation. For example, at 850°C application of 1000 grams for 15 minutes produced a plastic deformation (elongation) of $\leq$ 0.2% over a 0.5 meter long hot zone. Breakage occurred, however, when heating the tape with current ($\sim$ 10A dc or ac rms) to reach the same tape temperature with a 500°C background furnace temperature. Even at much lower tension forces the plastic flow was prohibitive: 2 to 3% after 15 mins. under a load of 150 grams, a necessary minimum for proper tape positioning. Predictably, the use of twice as thick tape (50 μm) has reduced the plastic deformation only by a factor of 2 to 3.

The flow effect was tentatively explained by nonuniform ohmic heating on Hastelloy grain boundaries having significantly higher resistivity than the grains themselves. High-power density dissipated at boundaries causing localized heating, grain slippage, and eventual breaking of the tape in analogy to the effects extensively studied for tungsten filaments used in incandescent lamps. In that case it was demonstrated that metallurgical control of the microstructure offers a satisfactory solution to the problem. Within the scope of this program, however, work on substrate metallurgy could not be justified.

In spite of the present lack of success the substrate ohmic heating still represents a desirable approach to fabrication of long tape conductors. It simply requires more work and a different reactor design.

2.4 Process Parameters

Carrier Gas: In static tape deposition experiments performed under the ERDA program, helium was used as the carrier gas. It was first

replaced by argon in the tape ohmic heating experiments since at normal (1 atm) pressure the thermal conductivity of Ar is much lower than that of He. Accordingly, the desired tape temperature could be achieved at a lower average power density in the tape. In these experiments, however, it was also observed that the coating rates on two sides of a horizontally-mounted tape were more uniform when using Ar than it was typical for He. Hence, Ar was ultimately adopted as the carrier gas. Representative tape section profiles obtained using Ar are given in Figure 8 . Deposit growth rates in Ar were reduced by 20 to 25% compared with the rates in He. This was due to much lower diffusivity of Ar. The improvement in coating uniformity was ascribed to lesser gas phase segregation in conditions of a nearly laminar flow in the horizontal deposition tube. The matter was, however, not studied systematically.

Deposition Temperature: Based on the data of Reference 5 the standard deposition temperature was chosen to be $T_d \simeq 850°C$. This choice was dictated by trade-offs between the achievable T_c (increasing with T_d up to 950°C), J_c (increasing with inverse T_d) and compositional uniformity along the deposition zone. A few deposition experiments at T_d = 880 to 900°C were also performed in the moving tape mode.

Deposition Zone Length: The deposition zone length, ℓ, was the distance between the masking tracks MT1 and MT2 in Figure 1. In the moving tape mode the deposit thickness at a given tape speed, v_t, increased with ℓ as shown in Figure 4 while the deposit uniformity decreased with increasing ℓ due to the existence of a compositional profile along the zone.[5] Such profiles were determined by measuring the cell edge, a_o, of the A15 single-phase static tape deposits. The profile used as a base for the choice of ℓ is given in Figure 5. The compromise deposition zone length chosen was $\ell \simeq 10$ cm.

Tape Speed: The standard tape speed chosen was ~ 0.75 m/hour. Double speed of ~ 1.5 m/hour was used in high delivery rate experiments aimed at producing long tape sections.

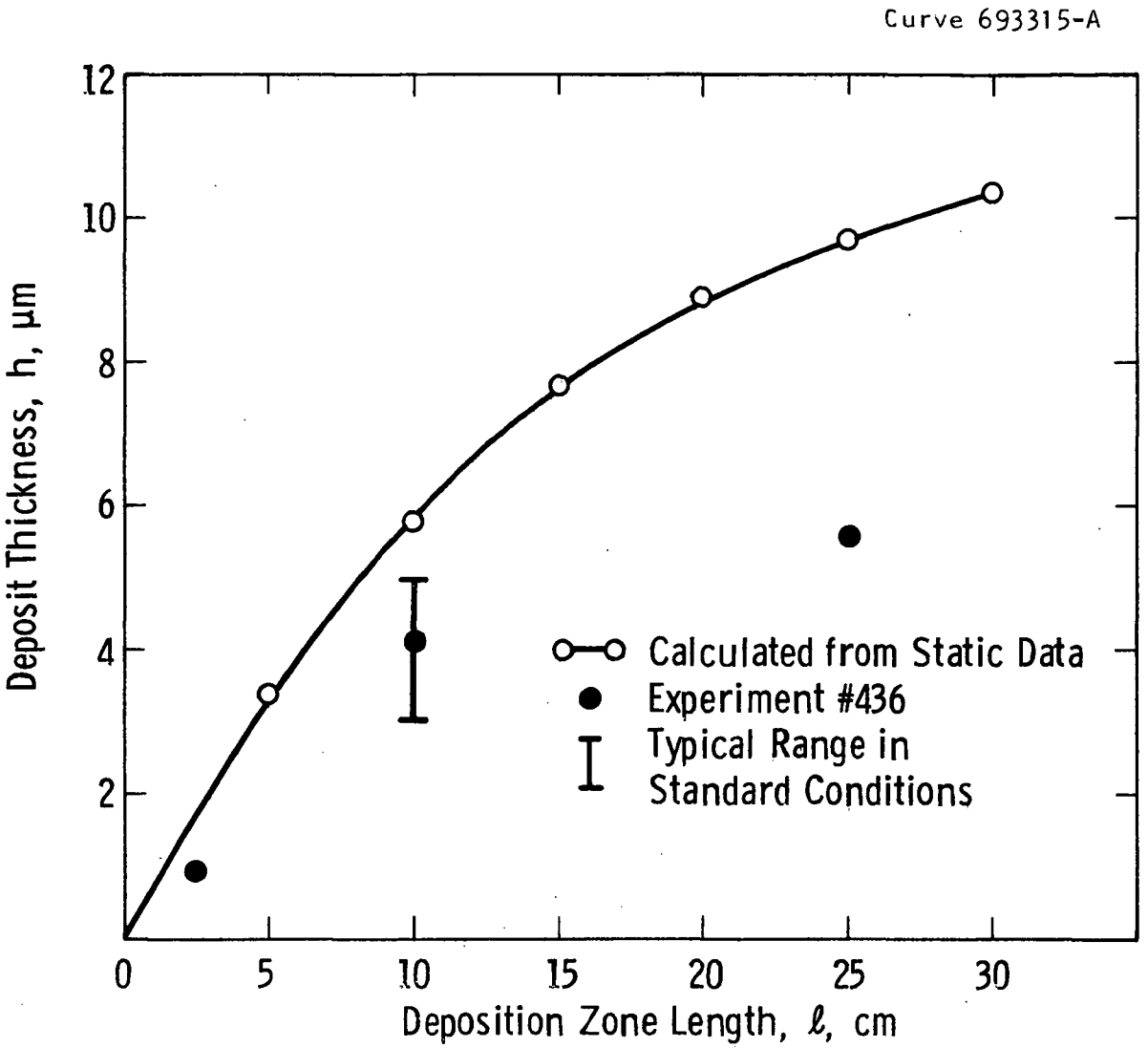

Fig. 4 – Deposit thickness, h, vs the deposition zone length, ℓ, in the moving tape mode; standard conditions of Table 2

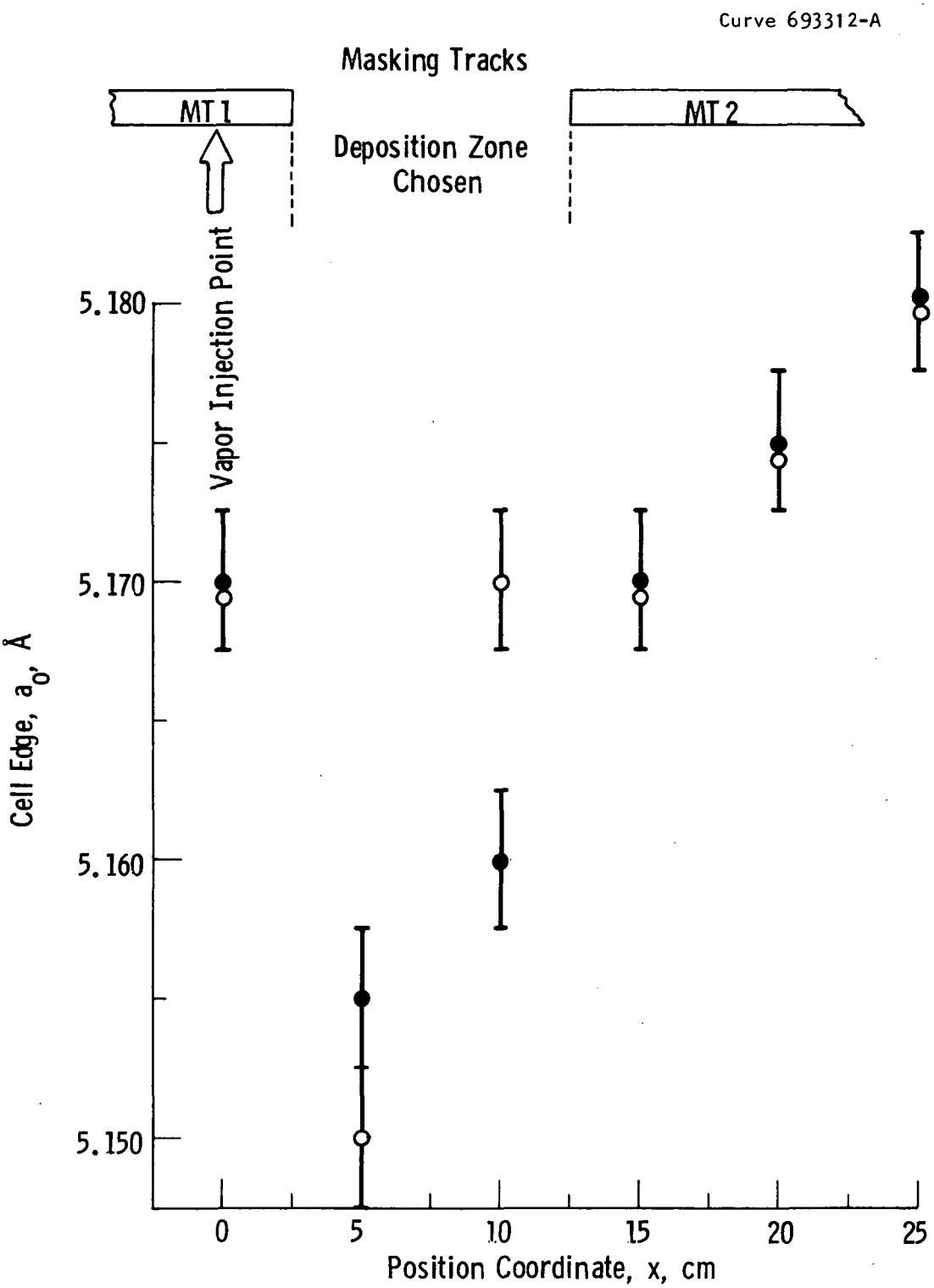

Fig. 5—Cell edge profile along the deposition zone, single phase A15; experiment 422 C. Open and full circles denote two sides of the tape

Delivery Rate: The standard delivery rate for Nb and Ge was kept on the same level as in static tape experiments described in Ref. 5 in spite of the change in produced chloride species (Section 2.2). The mass of niobium transported toward the deposition zone was ∿ 9.3 gram/hour. The mass of germanium was ∿ 2.1 grams/hour. It was varied between 1.6 and 2.4 grams/hour in experiments aimed at optimizing the deposit composition. In experiments testing the fabrication of up to 10 meters long tape sections double rates were used, i.e., ∿ 18.5 and 4 grams/hour for Nb and Ge respectively.

Summary: The standard deposition parameters used in the moving tape experiments are summarized in Table 2.

Table 2

Deposition Parameters in the Moving Tape Mode

Parameter	Unit	Standard Value	Double Rate Value
Vapor mixing temperature	°C	∿ 400	∿ 400
Deposition temperature, T_d	°C	$850\ ^{+10}_{-20}$	$850\ ^{+10}_{-20}$
Argon carrier flow rate (main line)	ℓ/min	8	8
Argon flow rate through vapor locks	ℓ/min	3 (per lock)	3 (per lock)
Hydrogen flow rate	ℓ/min	12	12
Nb mass delivery	g/h	9.3	18.5
Ge mass delivery	g/h	$2.1\ ^{+0.3}_{-0.5}$	4
Deposition zone length, ℓ	cm	10	10
Tape speed, v_t	m/hour	0.75	1.5
Tape width	cm	0.6	0.6
Substrate thickness	μm	50	50
Deposit thickness, h (per side)	μm	4 ± 1	4 ± 1

2.5 Homoepitaxial Deposition

In a recent publication Dayem et al. presented data indicating that stoichiometric Nb_3Ge may grow epitaxially on polycrystalline A15 substrates, such as Nb_3Ir, which have matching cell edge values.[10] Newkirk at LASL suggested that if the above is true then homoepitaxial deposition on Nb_3Ge should also occur.[11] One could initially nucleate the stable, Ge-deficient, A15 phase and then very gradually decrease the ratio s = Nb/Ge in the vapor phase to shift the deposit composition and attain the 3:1 stoichiometry. A high T_c, uniform Nb_3Ge phase should thus eventually grow on top of a transition layer having a more or less steep compositional gradient normal to the surface. The Nb-Ge composition varies along the deposition zone of the moving tape CVD reactor. Homoepitaxial deposits could be grown were the tape substrate moving in the direction of decreasing s (which was, incidentally, the standard direction adopted in this program).

In experiments 437 and 438 an attempt was made to verify the above suggestion. Static tape run 437 was made to determine the growth rate, $h_t(x)$, and cell edge $a_o(x)$ profiles at $T_d \simeq 850°C$ over a length of 40 cm. The Marshall furnace (Figure 8, Appendix II) was reattached to the reactor for this purpose. The growth rate profile was found to be too flat to be practical. In consequence, in run 438 the temperature was increased to T_d = 900 to 920°C to make the profile steeper. The $h_t(x)$ data indicated that in the moving tape mode 60% of the total layer thickness would grow in the first 10 cm of the deposition zone adjacent to the vapor injection point (Figures 1 and 5) where the composition change would be small. The remaining 40% would have a significant (desired) composition gradient. Epitaxial growth conditions were then modeled by linearly decreasing the s value during the deposition from s = 8 to s = 3 at a rate of -0.3/min. No improvement of the deposit properties was observed when comparing with the standard samples grown at a constant s = 3.0 and 3.6. Hence, no further work was expended in this direction. However, the experiments were not complete enough to draw any conclusion about the basic possibility of homoepitaxial deposition.

2.6 Deposition of Thin and Layered Films

Films of Nb_3Ge grown over short periods of time to produce thicknesses in the submicron range should have finer microstructure and less columnar morphology than standard thickness deposits. Such films could be compared with thin sputtered films. In experiments 452 and 455 thin films were grown in the static mode by manually drawing the tape into the deposition zone, holding it there for a predetermined length of time and then quickly pulling it out of the furnace. Deposition conditions were otherwise standard. Properties of such films are discussed in Sections 5.2 and 5.3. Significant increase of critical-current density was observed. Crude attempts were also made to form multilayered structures of such thin films. Since the CVD reactor had no provisions for layering by introducing intermediate, thin, nonsuperconducting layers three types of experiments were performed:

1. Periodic variation of s ratio.
2. Introduction of intermediate layer material available for delivery in vapor form.
3. Periodic interruption of deposition process.

In run 446 layering on static (immobile) Hastelloy substrate was attempted by periodically introducing bursts of additional $GeCl_4$ to form a stack of alternating Nb_3Ge and nonsuperconducting Nb_5Ge_3 layers of various thicknesses. In run 447 the same was repeated under moving tape conditions. In run 448 silicon growth rates were determined using 3% silane, SiH_4, as a source. Silicon could be used as a material to form nonsuperconducting layers. In static run 449 bursts of normal delivery mixture, $NbCl_5 + GeCl_4$, were periodically introduced to determine whether random Nb_3Ge nucleation will start with each layer thus breaking the columnar growth habit.

Finally, in run 452 G, H renucleation was attempted by periodically pulling the substrates in and out of the deposition zone. In all of the above runs, standard (reference) Nb-Ge samples have also been

prepared for the sake of comparison with layered deposits. Results of these layering experiments remained inconclusive.

3. TAPE SUBSTRATES

3.1 General Requirements and Description

A substrate for magnet tape conductors should have the following properties:

1. Thermal expansion (contraction) compatible with that of the deposit.
2. High elastic modulus and high strength.
3. High electrical and thermal conductivity at low temperatures.
4. Strong bonding to the deposit without formation of a thick diffusion layer.
5. Chemical compatibility with the superconductor deposition process.
6. Minimum thickness to insure a small minimum bending radius.

In the present work Hastelloy B tape substrates offered a practical compromise between several of the conflicting requirements. Accordingly, Hastelloy B* was used throughout this program as the standard substrate material for Nb_3Ge deposition. In addition, in a limited number of experiments Nb-1% Zr and Ta tape substrates were used to evaluate the effects of strains in Nb_3Ge that were induced by differential thermal contraction.

In static tape experiments the Hastelloy B tape used was 1.27 cm (0.5 inch) wide and ≃ 50 μm (2 mil) thick. Such tapes have been coated

*Ulbrich Stainless Steel and Specialty Metals, Inc., P. O. Box 294, North Haven, CT 06473.

on one side only. In the moving tape mode tapes 0.6 cm (∿ 0.25 inch) were used. The standard thickness was again $h_s \simeq 50$ μm, i.e., as delivered. The original tape length was up to several hundred meters per section. Also, sections of 25 μm thick Hastelloy B tape were fabricated in-house by rolling, annealing and slitting the 50 μm thick, 1.27 cm wide strips. The total length was ∿ 1000 meters. The thickness tolerance was within < ± 10% for most strips. The starting material thickness tolerance was zero to +10%.

The Nb-1% Zr and Ta substrates were also 0.6 cm wide. The Nb-Zr tape thickness was $h_s \simeq 75$ μm, the Ta tape was ∿ 50 μm thick. Table 3 gives qualitative performance ratings for the three above materials used as substrates for CVD of Nb_3Ge.

Table 3

Substrate Material Performance Rating

Material	Hastelloy B	Nb (Nb-1% Zr)	Ta
Thermal contraction compatibility	poor produces $\varepsilon \simeq -0.6\%$ compressive strain in Nb_3Ge	good, $\varepsilon \simeq -0.04\%$	fair to good $\varepsilon \simeq +0.04\%$
Elastic modulus and tensile strength	high	fair	high
Electrical and thermal conductivity	low	high	high
Bonding	excellent, but Ni diffuses into Nb_3Ge	poor to fair	poor to fair
Chemical compatibility with CVD	very good	poor - hydride formation	poor - hydride formation

In the following sections the substrate properties and performance are discussed in some detail. It is already clear from Table 3, however, why these three materials have been considered.

3.2 Properties of Hastelloy B

Typical composition and some properties of Hastelloy B are given in Table 4.

Table 4

Typical Properties of Hastelloy B
(Composition: 66% Ni, 24% Mo, 4 to 6% Fe)

Parameter	Unit	Value at 293 K	Value at 20 K
Modulus of elasticity, E,[14]	10^{11} newton/m^2	1.8 to 2.2	2.2 to 2.3
	10^6 psi	26 to 30	32 to 33
Tensile strength[14]	10^8 newton/m^2	8.3 to 8.9	$\sim$ 15
	10^3 psi	120 to 130	$\sim$ 220
Yield strength (0.2% offset)	10^8 newton/m	3.9	?
	10^3 psi	56	?
Thermal expansivity	SEE SECTION 3.4		
Electrical resistivity, ρ	10^{-6} Ω-cm	135	120
Thermal conductivity, K,[12]	W m^{-1} K^{-1}	?	$\sim$ 10

The microstructures of Hastelloy B tapes are shown in Figure 6.

3.3 Niobium and Tantalum, Hydriding

Niobium and tantalum properties are given in Table 5. Tapes of these materials have been used only in strain effect related experiments. The use of both Nb-1% Zr and Ta was difficult due to the hydrogen

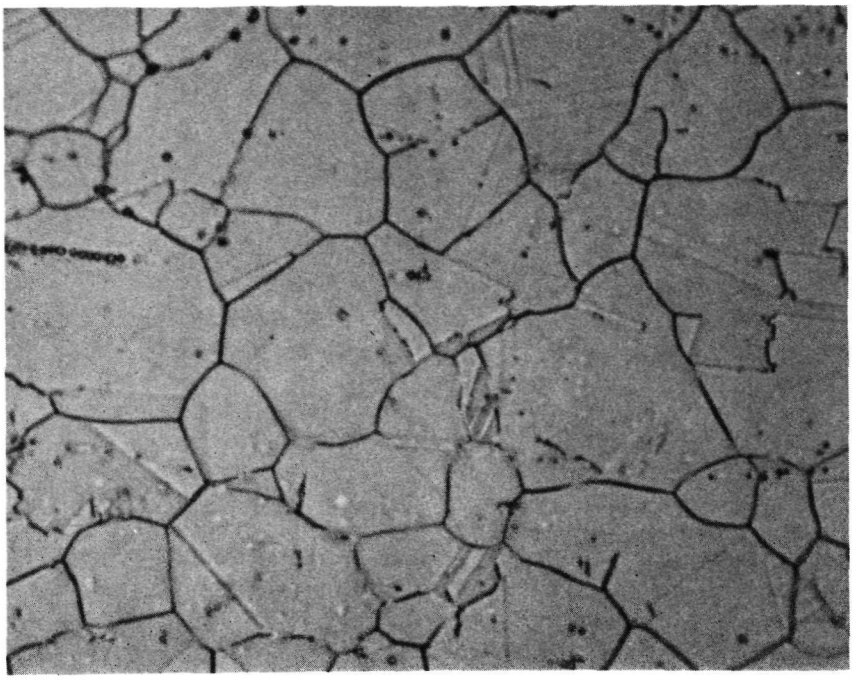

(a)

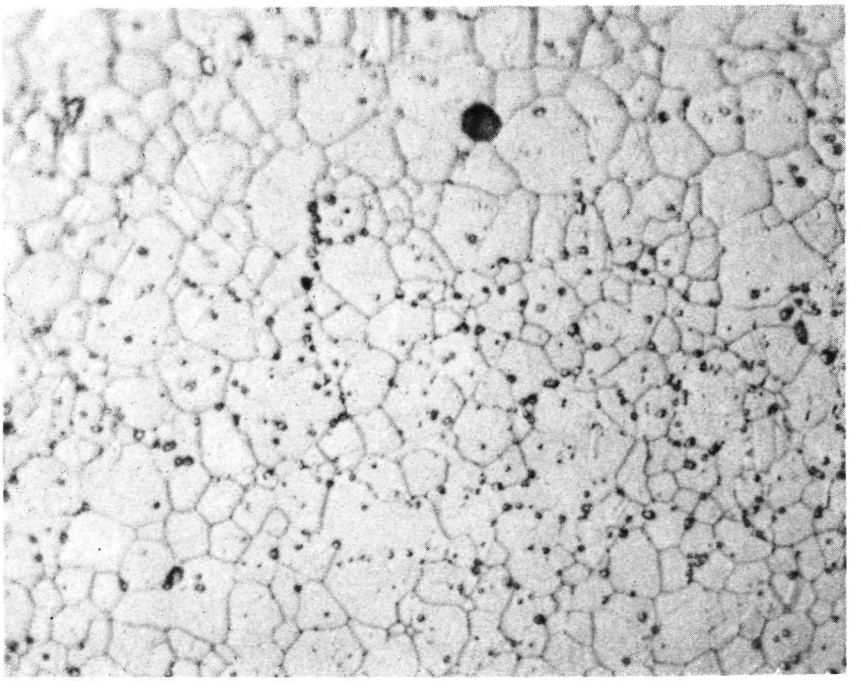

(b)

Figure 6 - The microstructure of Hastelloy B tape substrates:
(a) 50 μm thick tape, average grain size ∿ 14 μm,
(b) 25 μm thick tape, average grain size ∿ 6 μm.

Table 5

Properties of Nb-1% Zr and Tantalum

Parameter	Unit	Values at 293K		Values at 20K	
		Nb	Ta	Nb	Ta
Modulus of elasticity, E[13]	10^{11} newton/m^2	1	1.9	NO DATA AVAILABLE	
	10^6 psi	15	27		
Tensile strength[+)]	10^8 newton/m^2	2.4	2.4		
	10^3 psi	35	35		
Yield strength[+)] (0.2% offset)	10^8 newton/m^2	1.4	2.2		
	10^3 psi	20	32		
Thermal expansivity	SEE SECTION 3.4				
Electrical resistivity, ρ[12]	10^{-6} Ω-cm	∿ 13	∿ 13	0.08	0.05
Thermal conductivity, K[12]	W m^{-1} K^{-1}	0.5	0.5	0.8	0.6 to 1.5

[+)] Kawecki-Berylco data.

embrittlement occurring when the substrate resided in the deposition zone and in the cooling zone of the CVD reactor.

It is well known that hydrogen solubility in Nb and Ta is very high even at low H_2 pressures, and that the material embrittlement results. The solubility increases with the inverse of the temperature as shown in Figure 7.[15] Embrittlement should thus occur especially at temperatures lower than the deposition temperature, i.e., in the cooling zone, unless the Nb_3Ge layer were able to protect the substrate. Whether embrittlement occurs at T_d = 850°C in the specific Nb_3Ge deposition condition was not clear. To check these points in static tape runs No. 422 and 423 the Nb-1% Zr and Ta substrates were quickly, in about 1 sec. time, drawn into the deposition zone ($T_D \simeq 850°C$). After 30 to 40 mins. deposition time to form a Nb_3Ge on all tape surfaces the samples were quenched by quickly pulling the tape out of the reactor. All eight samples tested (4 Nb and 4 Ta) turned very brittle and broke after one bend thus clearly indicating that hydrogen diffused through the forming Nb-Ge layers (having final thicknesses ranging from 2 to 15 μm, depending upon the conditions of the experiment). Since slow cooling of the sample in the moving tape mode could only contribute to further embrittlement it became clear that the use of Nb or Ta as a substrate for practical conductors made by the present CVD process will not be feasible unless a hydrogen diffusion barrier is formed on the substrate. In experiment No. 424 performed in the same manner as 422 and 423 tantalum substrates coated with a 3000 to 5000 Å thick layer of nickel were tested with negative results. Finally, in run No. 433 a Ta substrate protected by 2 to 3 μm layer of sputtered copper was tested successfully. An observable embrittlement did not occur even in the moving tape mode, i.e., upon slow cooling of the sample. Hence, the feasibility of using Ta (or Nb) copper-coated substrates for practical Nb_3Ge conductors was convincingly demonstrated.

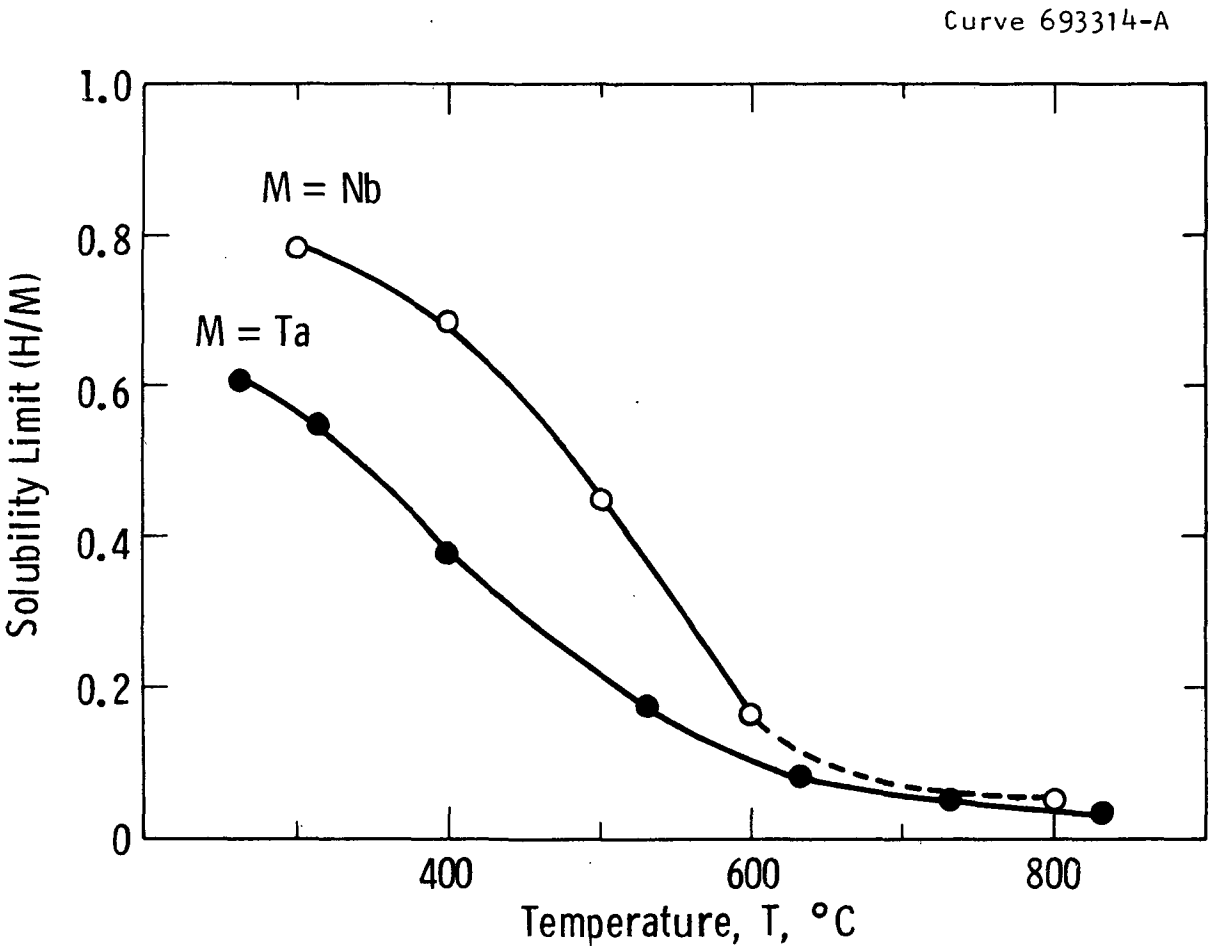

Fig. 7—Solubility of hydrogen in niobium at 1 atm H_2 pressure; experimental data

3.4 Minimum Bending Radius

Brittle A15 superconductors degrade significantly when strained. Tensile straining eventually leads to cracking. Both, compressive and tensile intrinsic strains lead to T_c, H_2 and J_c degradation below the cracking limit. In the case of Nb_3Sn a ballpark figure of $\varepsilon_o \leq |\pm 0.2\%|$ can be assumed as an intrinsic strain limit above which J_c deterioration occurs.[16,17] No data exist yet for Nb_3Ge so that Nb_3Sn results serve as a guideline. Strains in the superconductor can be grossly divided in two categories:

1. Strains resulting from externally-applied stress due to bending, pulling, cooldown on mandrels and the Lorentz force.
2. Internal strains in the composite conductors due to fabrication process and, especially, to differential thermal contraction.

In conductors for high-field laboratory magnets having a small bore the admissible strain level determines the substrate thickness for a given bending radius and vice versa. The unidirectional strain at outer surfaces of a symmetrical tape conductor, i.e., one having on each side of the substrate a superconducting layer of equal thickness, is $\varepsilon = \pm \left(\frac{1}{2} h_s + h\right)/r$ where h_s is the substrate thickness, h the superconductor thickness and r is the bending radius. A desired value of r is $\lesssim$ 1 cm which allows construction of magnets having a bore of 2.5 cm (1 inch). For a h_s = 25 μm substrate $\varepsilon \cong \pm$ 0.18%, an acceptable number. Hence, deposition on such thin substrates was attempted. However, the observed plastic deformation (Section 2.3) under ohmic heating and deformations (transverse curling) due to thermal contraction of slightly assymetrical tapes prompted the adoption of h_s = 50 μm. With such substrates a minimum bending radius of $\sim$ 1.5 cm could be obtained for an otherwise unstrained superconductor.

3.5 Thermal Contraction Mismatch

The thermal expansivity of the substrate materials under discussion is approximated by the following empirical expressions:[12]

Hastelloy B:

$$\frac{\Delta L}{L_o} = -0.184 + 2743 \times 10^{-4}\, T + 1.292 \times 10^{-8}\, T^2 - 4.044 \times 10^{-10}\, T^3$$

(±7%, entire temperature range),

Niobium:

$$\frac{\Delta L}{L_o} = -0.125 + 5.164 \times 10^{-4}\, (T - 100) + 9.858 \times 10^{-7}\, (T - 100)^2$$

$$- 1.525 \times 10^{-9}\, (T - 100)^3$$

(±3% at 100 < T < 293K)

$$\frac{\Delta L}{L_o} = 7.265 \times 10^{-4}\, (T - 293) + 1.026 \times 10^{-7}\, (T - 293)^2$$

$$- 1.032 \times 10^{-11}\, (T - 293)^3$$

(±3% at 293 < T < 1200K)

Tantalum:

$$\frac{\Delta L}{L_o} = 6.308 \times 10^{-4}\, (T - 293) + 9.706 \times 10^{-8}\, (T - 293)^2$$

$$- 2.545 \times 10^{-11}\, (T - 293)^3$$

(±3% at 293 < T < 1100K)

In these expressions L_o is the length at 293K, ΔL the length increment and T is in degrees Kelvin.

The thermal expansivity of Nb_3Ge was given in Ref. 9 for the temperature range $293 \leq T \leq 1033K$, and in Ref. 18 for $4.2 \leq T \leq 675K$. Maximum thermal contraction mismatch between Nb_3Ge and substrate should occur when cooling the conductor from the deposition temperature down to the cryogenic application temperature T. The resulting strain in the x-y film plane should be

$$\varepsilon = \varepsilon_x = \varepsilon_y = \frac{\Delta L}{L_o}_{(Nb_3Ge)} - \frac{\Delta L}{L_o}_{(substrate)}$$

calculated for the above temperature range. Table 6 gives the $\Delta L/L_o$ and resulting ε values for $T_d = 850°C$ (1123K) and T = 0 K, determined from the above empirical expressions and/or graphs and numerical data from Refs. 12, 9, 18.

Table 6

Thermal Contraction Between 1123K and 0 K and the Resulting Mismatch Strain

Material	$\frac{\Delta L}{L_o}$	Nb_3Ge Mismatch Strain, ε, %
Nb_3Ge	7.9×10^{3}	--
Hastelloy B	14.0×10^{-3}	-0.6
Niobium	8.3×10^{-3}	-0.04
Tantalum	7.5×10^{-3}	+0.04

Data of Table 6 suggest that the Nb_3Ge properties should be degraded when using Hastelloy B as a substrate. Due to superposition of mismatch strains and strains induced by bending, the inner radius layer will be degraded more than the outer layer where the strains subtract.

Because of the nonlinearity of the J_c vs intrinsic strain curve[17] the inner layer degradation due to bending will be more significant than in the absence of thermal contraction prestressing. In the case of Nb and Ta substrates mismatches are reasonably small and the strain level at zero field is a function of the actual radius of the magnet coil.

4. SAMPLES

4.1 Macrostructure, Labeling

As already stated in Section 3.1 samples prepared in static tape experiments were deposited on one side of 1.27 cm (0.5 inch) wide and 50 μm thick Hastelloy B substrates. The Nb_3Ge layer thickness ranged from 2 to 20 μm. The samples were slightly bent (curled) around the major tape axis with the coated surface convex due to thermal contraction mismatch. Such tapes are labeled Type I in the following text. In the moving tape mode (Type II samples) Nb_3Ge layers were deposited on all surfaces of Hastelloy substrate tapes 0.6 cm wide. The layer thickness has been determined from micrographic sections using an optical microscope. Nominal thickness was 4 ± 1 μm per side, but varied considerably depending upon conditions of deposition, process parameters fluctuation, etc. Scanning electron microscopy (SEM) was used to measure thicknesses of the order of 1 micrometer and below. Figure 8 shows results of thickness measurements plotted as two typical sample section profiles, one symmetrical and one asymmetrical, i.e., having one side layer thicker than the other. Such asymmetry has been relatively common as shown in Table 7 and was due to gas phase stratification discussed in Section 2.4. Much thicker layer around the tape edges seen in Figure 8 was a common feature of all samples. The thick edges contributed no more than 2 to 4% to the total Nb_3Ge cross section and could, therefore, be neglected in the critical-current density determination.

Tape samples used for critical-current density measurement were coated on both sides with 5 to 10 μm of high-purity copper to stabilize against flux jumps. Copper was deposited either by sputtering or by electron beam evaporation. Adhesion of both types of Cu layers was firm upon cycling between room temperature and 4.2 K provided that the Nb_3Ge surface was precleaned by backsputtering in the case of sputtered layers.

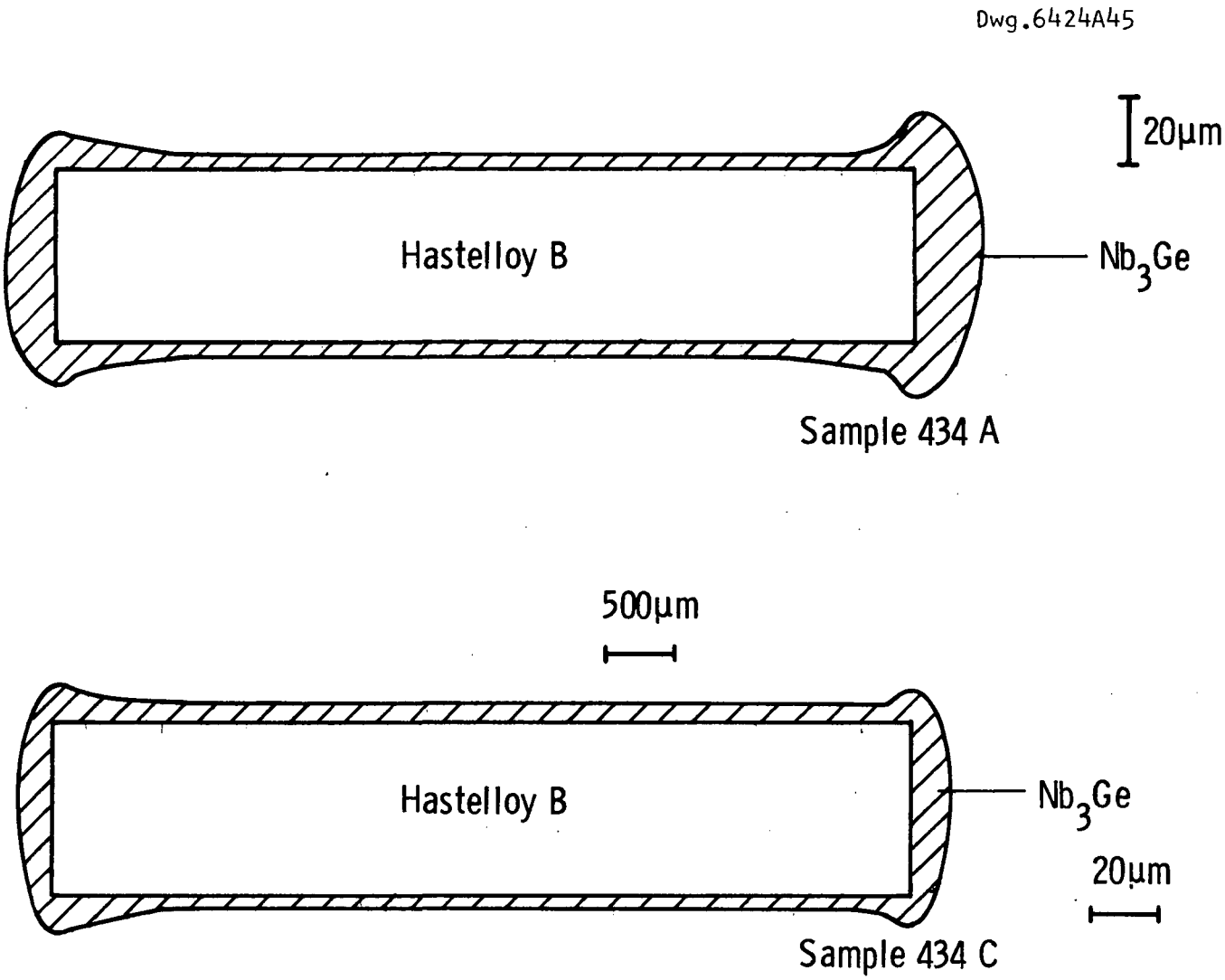

Fig.8—Thickness profiles of typical Type II Nb_3Ge tapes. The horizontal scale is compressed 25 times (except for the layer thickness)

Table 7

Random Selection of Nb_3Ge Thickness Data,
(Type II Tapes)

Sample Number	Thickness, h, in μm		
	Side 1	Side 2	Total
434 A	4.2 to 4.4	4.0	8.2 to 8.4
434 C	5.0 to 5.4	3.3 to 3.5	8.3 to 8.9
435 C	2.0 to 2.2	3.9 to 4.5	5.9 to 6.7
439 AU	5.6	3.6	9.2
439 BD	5.6	4.7	10.3
439 CU	5.2	3.1	8.1
439 DU	4.8	3.2	8.0
443 G	2.5	5.1	7.6
443 H	3.7	4.7	8.4
440 (5 m long tape)			
end 1	3.0	3.2	6.2
end 2	2.0	4.5	6.5
444 (10 m long tape)*			
444-2	2.0	3.1	5.1
444-4	2.3	3.2	5.5
444-6	3.7	5.0	8.7
444-8	2.4	4.6	7.0
444-10	3.9	4.3	8.2
444-12	3.9	4.9	8.8
444-14	4.3	5.9	10.2
MEAN	3.2	4.4	7.6
TOLERANCE	-50%	-23%	-36%
(4 μm nominal)	+8%	+48%	+28%

*h measured every 50 cm

Short specimens, up to 10 cm long were copper-coated by sputtering, longer ones, up to 35 cm, by E-beam evaporation. At equal thickness the sputtered copper was more effective in stabilizing the samples. A systematic comparison of Cu resistivity ratios was not made.

The useful sample length was 1 to 5 cm for Type I samples because of compositional variations along the tape. Type II tapes were up to 10 m long. Typically, when evaluating the effect of process parameters upon the sample properties specimens 10 to 30 cm long have been prepared. In such a case the Latin or Greek characters following the run number indicated a specific set of parameters, e.g., 439 B was a label for the variant B of run 439. Some long tapes were sectioned into 25 or 50 cm long specimens to allow characterization. In such cases additional arabic numerals denoted the consecutive section. For example, label 444-10 denoted 10th section of tape prepared in Run 444. Labeling of Type I was analogous: additional arabic numerals denoted the sample positions in the deposition zone at 5 cm intervals.

4.2 Phases and Microstructure

Type II Nb_3Ge samples for high-field application contained 5 to 10% of Nb_5Ge_3 tetragonal phase dispersed in the A15 matrix and serving as flux pinning centers. Transmission electron microscopy (TEM) revealed that the size and spacing of Nb_5Ge_3 particles decreased with deposition temperature.[19] This is illustrated in Figure 9 obtained in a separate study program.* The A15 grain size decreased only slightly with T_d but very dramatically with the layer thickness, h. Figure 10 shows a TEM micrograph of a typical 5 m long tape deposited at T_d = 850°C. In this $\sim$ 5 μm thick layer the Nb_5Ge_3 particle size is 100 to 300 Å, mean spacing is undefined and mean grain size of A15 matrix is $\bar{d}$ = 1400 Å.

Type I samples deposited at T_d = 900°C were doped with Nb_5Ge_3, NbN and NbC to compare the effectiveness of flux pinning on various second

*Air Force Office of Scientific Research Contract No. F44620-74-C-0042.

Curve 693350-A

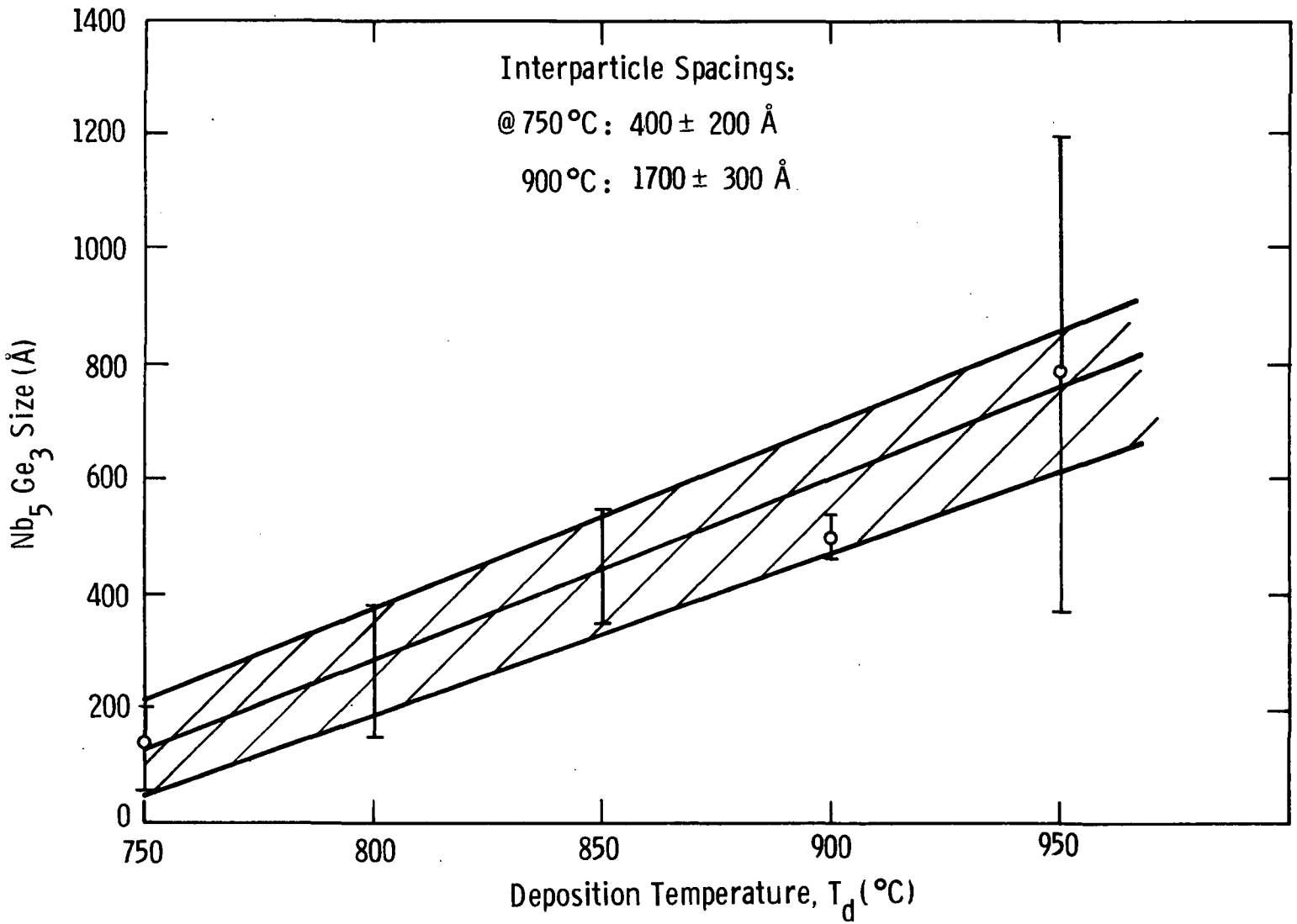

Fig. 9 – The Nb_5Ge_3 mean particle size in A15 Nb_3Ge matrix vs the deposition temperature, T_d

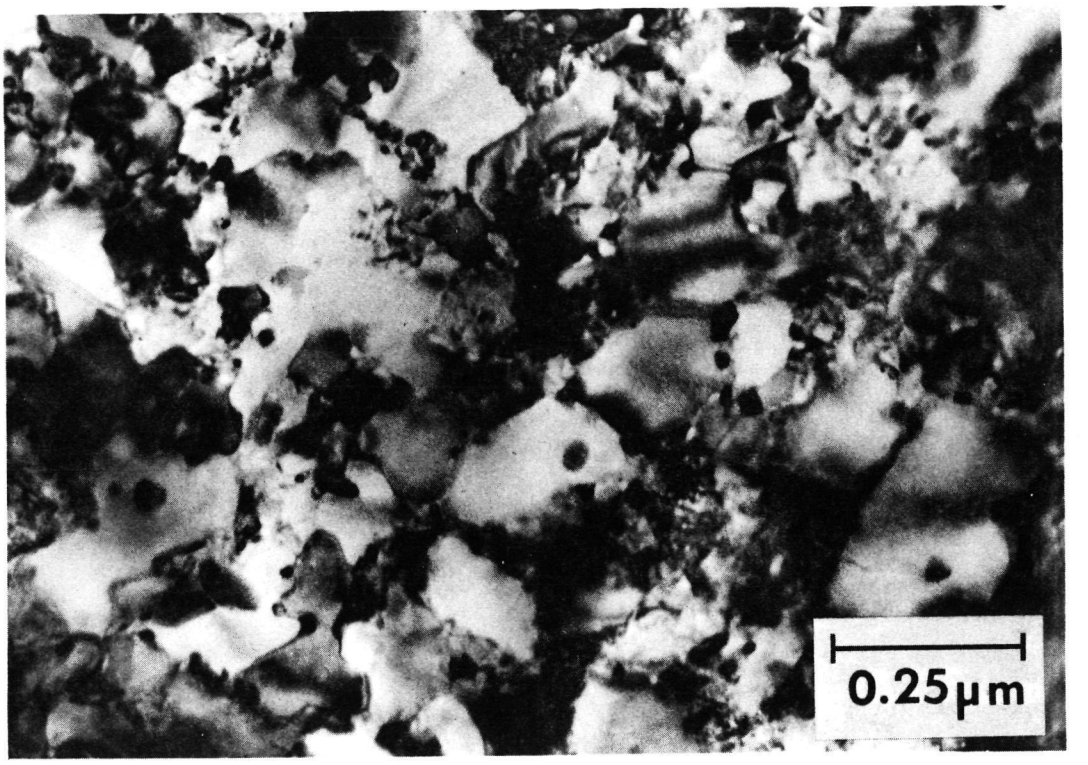

Fig. 10 TEM micrograph of tape #435 (Type II)

phases. The pertinent phase and microstructure data were already published.[7]

All the deposits exhibited columnar grain structure with a (200) texture that was more pronounced in Type I than in Type II samples (see Section 5.3).

At the boundary between Nb_3Ge and Hastelloy B a diffusion layer was invariably formed due to nickel diffusion. The Ni_3Nb and NiNb phases have been observed in Debye-Scherrer patterns.[5] Auger spectroscopy profiles determined for Type I samples deposited at 900 and 1000°C indicated that the diffusion layer was about 1 μm thick.[5] Hence, the effective superconductor thickness was less that the total deposit thickness.

5. SUPERCONDUCTING PROPERTIES

5.1 Critical Temperature

Methods used in this work to determine critical temperatures, T_c, were discussed in Ref. 5. Routine characterization, with ± 0.2 K accuracy, has been performed resistively using the standard four-point method and calibrated Ge-thermometers. Inductive (susceptibility) and magnetization measurements verified the consistency of resistive results. Precision characterization, ± 0.05 K, was performed by extrapolating the upper critical field vs temperature dependence H_{c2} (T) determined in pumped hydrogen at the National Magnet Laboratory.

The dependence of T_c upon the deposition temperature was determined for Type I samples containing Nb_5Ge_3 in concentrations necessary to insure necessary flux pinning. In Figure 11 the T_c (T_d) curve is compared with the highest T_c data obtained for single A15 phase samples. Generally, the second-phase containing samples had T_c degraded by 0.5 - 1 K compared with pure A15 samples. At T_d = 850°C the representative mid-point value was $T_c \simeq$ 20.0 to 21.0 K.

The effect of doping with impurity second phases such as NbN, NbC and also O_2 introduced when doping with carbon using CO_2 is summarized in Figure 12 for Type I samples deposited at T_d = 900°C.[20] In the impurity concentration range of 0.2 to 0.5 wt. %, necessary to insure flux pinning, the T_c degradation was comparable or greater than in the case of Nb_5Ge_3-doping.

Table 8 gives a representative selection of critical temperature results obtained for Type II tape samples deposited at T_d = 850°C. The average critical mid-point temperature was $T_c \simeq$ 20 K with an average transition width of 1.5 K, consistent with Figure 11. The critical temperature profiles along tapes of 5 and 10 meter length are shown in

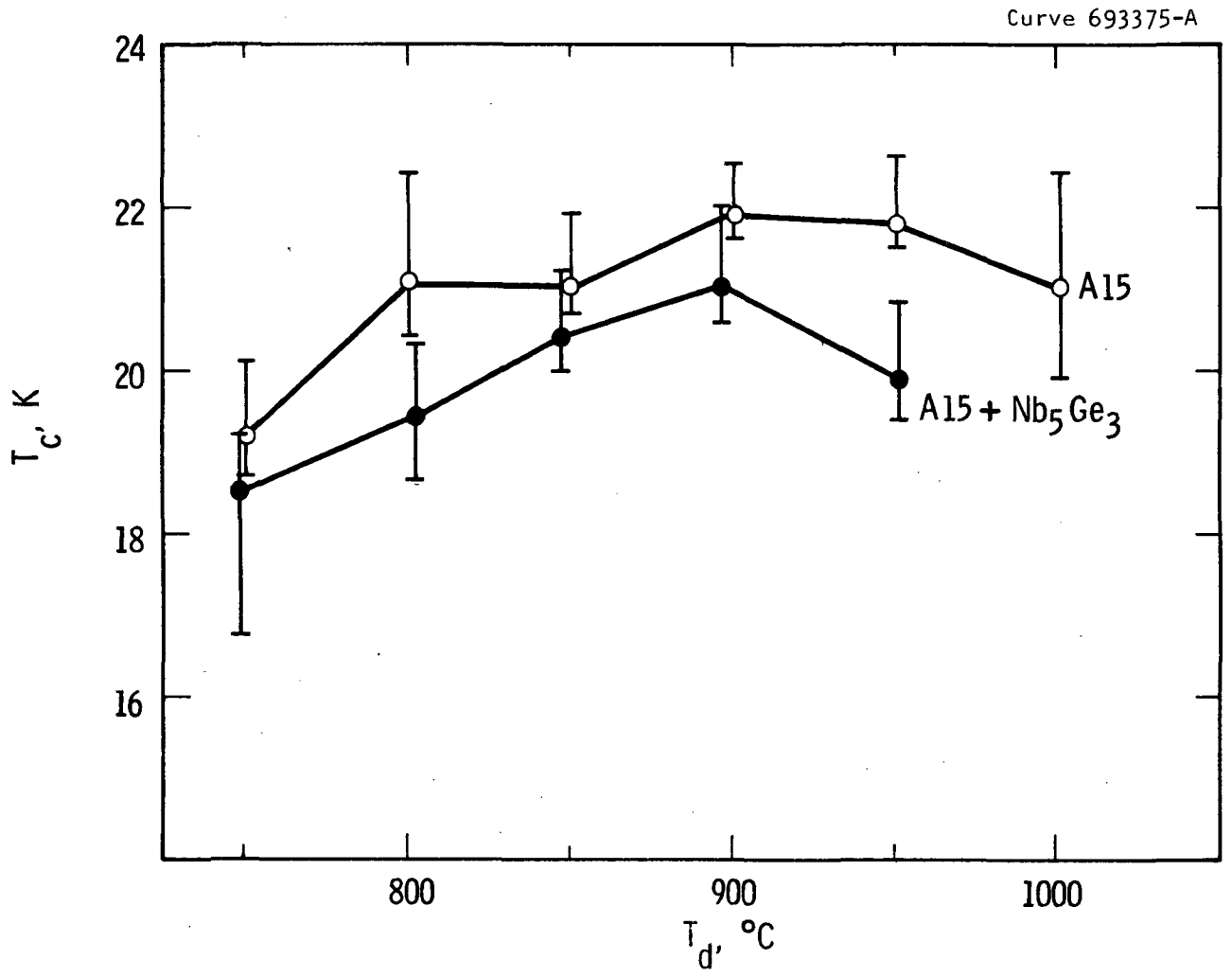

Fig. 11 – Highest achieved critical temperature, T_c, vs the deposition temperature, T_d for Type I samples. The bars indicate the width of the superconductive transition

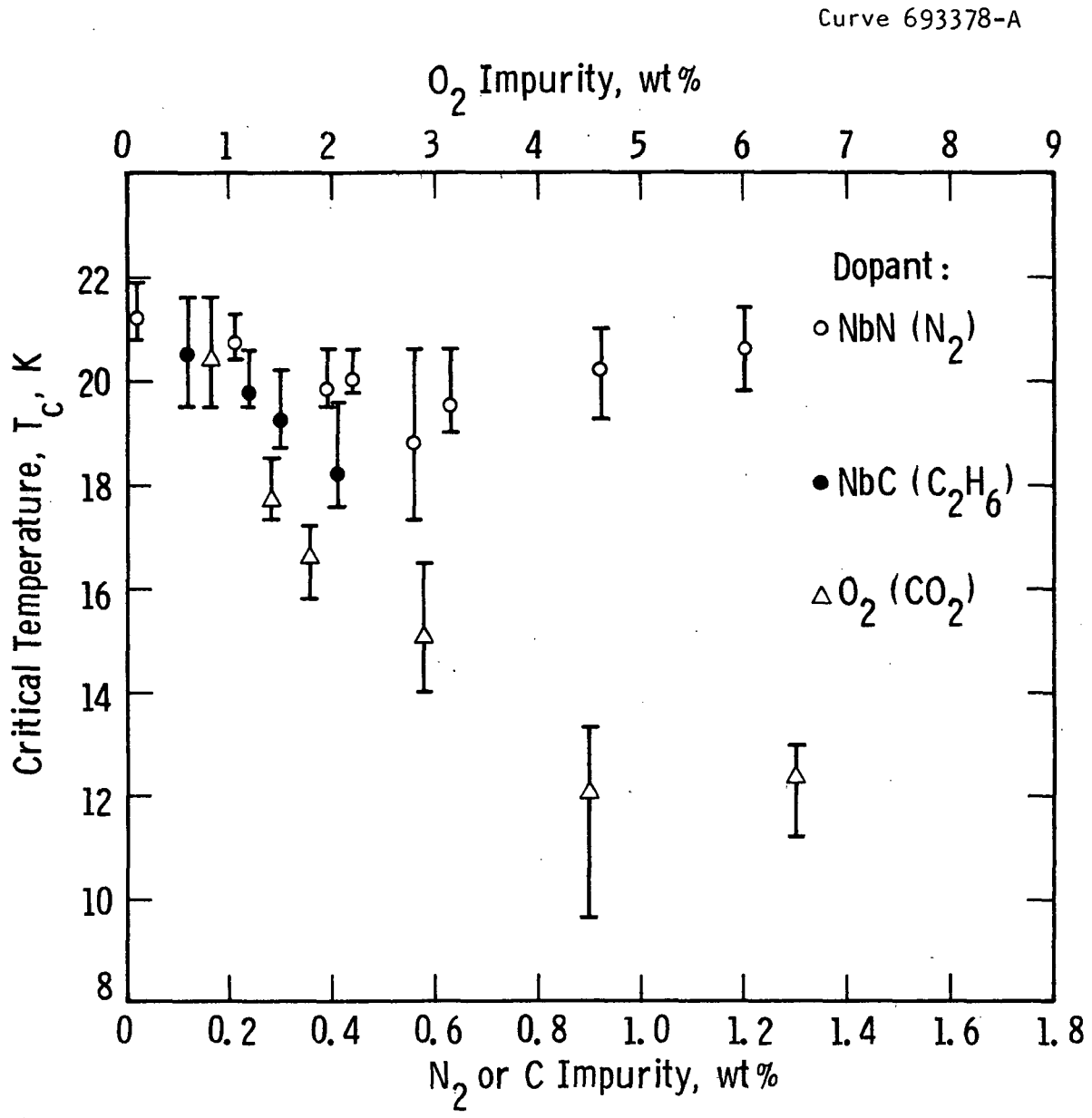

Fig. 12— Critical temperature vs. impurity concentration. Type I samples, T_d = 900° C

Table 8

Critical Temperatures of Type II Samples
(Degrees Kelvin)

Sample Number	Resistive Measurement, Ge-Thermometer			H_{c2} (T) Extrapolation		
	Onset	Midpoint	Tail	90% ρ_n	50% ρ_n	10% ρ_n
432 CU	20.4	20.1	19.7			
432 DU	21.1	19.9	18.9			
433 D (Cu/Ta)	19.6	19.0	18.4			
433 D	21.1	20.3	19.8			
439 DD	20.9	20.1	19.4	20.40	19.80	19.45
440 (end 2)	20.7	19.9	19.3	20.45	20.35	20.20
441 (end 2)	21.5	20.3	19.3			
442 CD	20.7	19.7	18.9			
443 E	21.1	20.3	19.5			
444-IJ	19.9	19.3	18.6			
450 (end 2)	21.3	20.1	19.1			
452 A	21.6	20.9	20.3			
MEAN	20.8	20.0	19.3			
452 C*	20.7	20.1	19.6	20.35	20.10	19.90
452 D*	20.7	20.2	19.7	20.55	20.20	19.85
452 F*	21.7	21.0	20.3	21.05	20.80	20.55

*Static, see Section 2.6

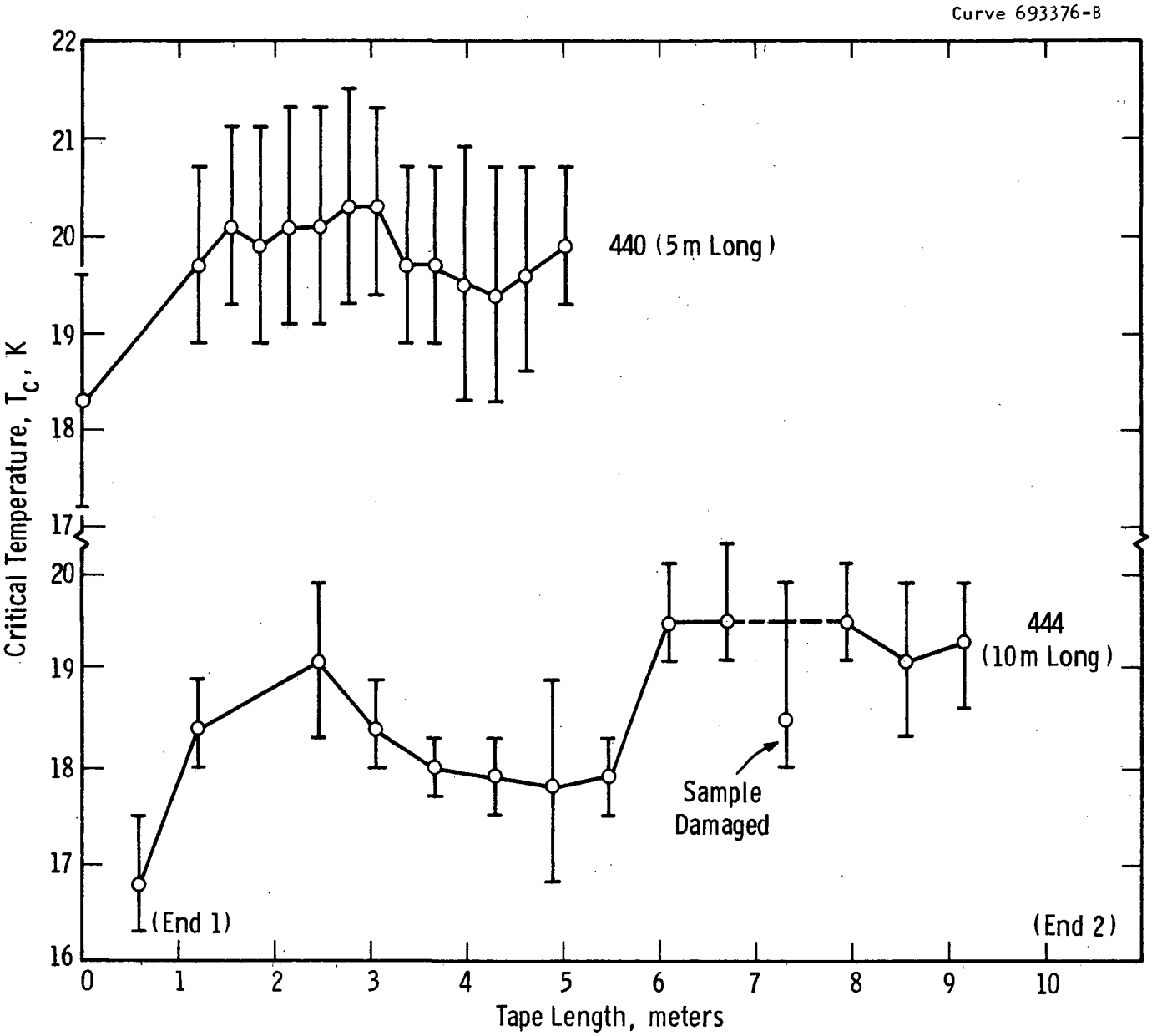

Fig. 13 – Critical temperature profiles along Nb_3Ge tape conductors

Figure 13. The variations were gradual and mostly monotonic indicating that properties of the tape depended upon slow, long-term fluctuation of the process parameters, most likely the s = Nb/Ge ratio, which was controlled manually. The control was apparently more erratic under the double rate conditions, i.e., in run 444. Degraded T_c's were always observed at the beginning of runs when the system has not yet attained equilibrium. After stabilization, under normal rate conditions such as in run 440, T_c fluctuated within 0.5 to 1 K.

5.2 Upper Critical Field

The upper critical fields have been determined between 14 and 20 K, i.e., in the pumped hydrogen range, using the four-point resistive method and either extrapolating to zero measuring current or operating with very low current densities of the order of 10^4 A m^{-2}. The temperature was accurate to ± 0.05 K. All measurements have been performed at the National Magnet Laboratory. The H_{c2} values have been determined from resistive transition curves using 90% of residual normal resistivity, ρ_n, as a criterion for defining H_{c2} at a temperature T. Below 14 K the H_{c2} values have been calculated from dH_{c2}/dT at $T \to T_c$[21] using the theoretical H_{c2} (T) dependence for dirty type II superconductor with no paramagnetic limiting.[21] Specifically, at 0 Kelvin:

$$H_{c2}\ (0) \simeq 0.69 \frac{dH_{c2}}{dT} T_c.$$

Table 9 summarizes all the dH_{c2}/dT data collected as well as the T_c values obtained by extrapolating H_{c2} (T) to zero field. Type I samples deposited at temperatures from 750 to 950°C and containing second-phase exhibited dH_{c2}/dT in the range of 1.95 to 2.15 tesla/degree with a calculated mean of 2.05 T/degree. Single-phase A15 samples showed a slightly higher mean of 2.14 kG/degree. All these samples were deposited on Hastelloy substrates and their thickness ranged from 3 to 15 μm. The above values of dH_{c2}/dT were distinctly below those obtained for 0.5 to

Table 9

Upper Critical Field Slopes $\lim_{T \to T_c} \frac{dH_{c2}}{dT}$

and Extrapolated Critical Temperatures
(Criterion: 90% ρ_n)

Sample Number	T_d	Phases	$\lim_{T \to T_c} \frac{dH_{c2}}{dT}$	T_c	Comments
	°C		tesla/degree	K	
86-9	750	A15	2.13	18.56	Type I
279-10		A15 + Nb_5Ge_3	2.12	18.59	
279-11		A15 + Nb_5Ge_3	2.02	17.43	
279-12		A15 + Nb_5Ge_3	2.07	19.77	
279-13		A15 + Nb_5Ge_3	2.16	19.88	
229-7	800	A15 + Nb_5Ge_3	2.06	20.28	
229-9		No Data	2.03	19.71	
229-11		A15 ?	2.13	20.00	
229-13		A15 ?	2.11	18.54	
228-9		?	1.90	19.05	
372-9	850	A15 + Nb_5Ge_3	2.01	21.16	
372-13		A15	2.03	21.61	
201-5	900	A15 + Nb_5Ge_3	2.00	20.80	
201-7		A15 + Nb_5Ge_3	2.04	21.00	
201-9		A15	2.14	21.15	
201-11		A15	2.07	22.05	
208-5		A15 + Nb_5Ge_3	1.95	21.90	
208-7		A15 + Nb_5Ge_3	2.05	20.60	
208-9		A15	2.15	20.90	
208-11		A15	2.18	21.80	
310-7		A15 + NbN + Nb_5Ge_3	2.06	20.78	
310-9		A15 + NbN	2.15	21.20	
310-11		A15 + NbN	2.08	20.98	
335-7		A15 + NbC + Nb_5Ge_3	2.09	18.18	
335-9		A15 + NbC	1.82	19.93	
244-5	950	A15	2.17	21.73	
254-7		A15 + Nb_5Ge_3	2.00	20.38	

(continued)

Table 9 (continued)

Sample Number	T_d	Phases	$\lim_{T \to T_c} \frac{dH_{c2}}{dT}$	T_c	Comments
	°C		tesla/degree	K	
439 DD	850	A15 + Nb_5Ge_3	2.19	20.40	Type II on Hastelloy
440 (end 2)		A15 + Nb_5Ge_3	2.22	20.45	
443 AD	850	A15 + Nb_5Ge_3	2.31	19.75	Type II on Ta/Cu
433 AU		A15 + Nb_5Ge_3	2.28	19.70	
455 KU	850	A15 + Nb_5Ge_3	2.13	19.55	2 h < < 1 μm
455 OU		A15 + Nb_5Ge_3	2.20	20.15	∿ 2 μm
452 C		A15 + Nb_5Ge_3	2.21	20.35	∿ 2 μm
452 D		A15 + Nb_5Ge_3	2.26	20.20	6 to 8 μm
452 F		A15 + Nb_5Ge_3	2.27	21.05	42 μm

1 μm thick Nb_3Ge sputtered on sapphire. The sputtered specimens had $dH_{c2}/dT = 2.4 \pm 0.1$ T/degree, and correspondingly higher H_{c2} (T) values. Since for Type I CVD samples the dH_{c2}/dT values were so remarkably constant and independent of the synthesis conditions, the calculated H_{c2} (T) values scaled well with T_c as shown in Figure 14 for 0 and 4.2 K. At 4.2 K with T_c = 20 K (90% ρ_n) H_{c2}'s were between 26.0 and 28.0 tesla while for sputtered samples having the same critical temperature 31 to 34 tesla would be typical.

Standard Type II samples (long tapes) had a slightly higher $dH_{c2}/dT \simeq 2.2$ T/deg, perhaps owing to an improvement in deposits uniformity obtained in the modified CVD reactor. At 4.2 K, H_{c2} = 29.0 to 29.5 T.

The question why dH_{c2}/dT is by 15 to 20% lower than in sputtered sampled is not yet fully answered. According to the Ginzburg-Landau theory:

$$H_{c2}\ (0) = A\ \rho_n\ \gamma\ T_c$$

where γ is the electronic coefficient of the specific heat which is proportional to the density of states and A is a constant. Hence:

$$\lim_{T \to T_c} \frac{dH_{c2}}{dT} \propto \rho_n\ \gamma.$$

It has been speculated earlier that fine-grained sputtered films have higher effective ρ_n than coarse-grained CVD deposits.[6] However, in fine-grained, very thin CVD films on Hastelloy that were prepared and studied under an independent program* dH_{c2}/dT = 2.0 to 2.1 T/degree (see, e.g., Table 9, sample 455 KU). It is therefore more likely that γ and, consequently, the density of states is lower in CVD films. For example, the density of states should be affected by strains induced in the

*Air Force Office of Scientific Research Contract No. F44620-74-C-0042.

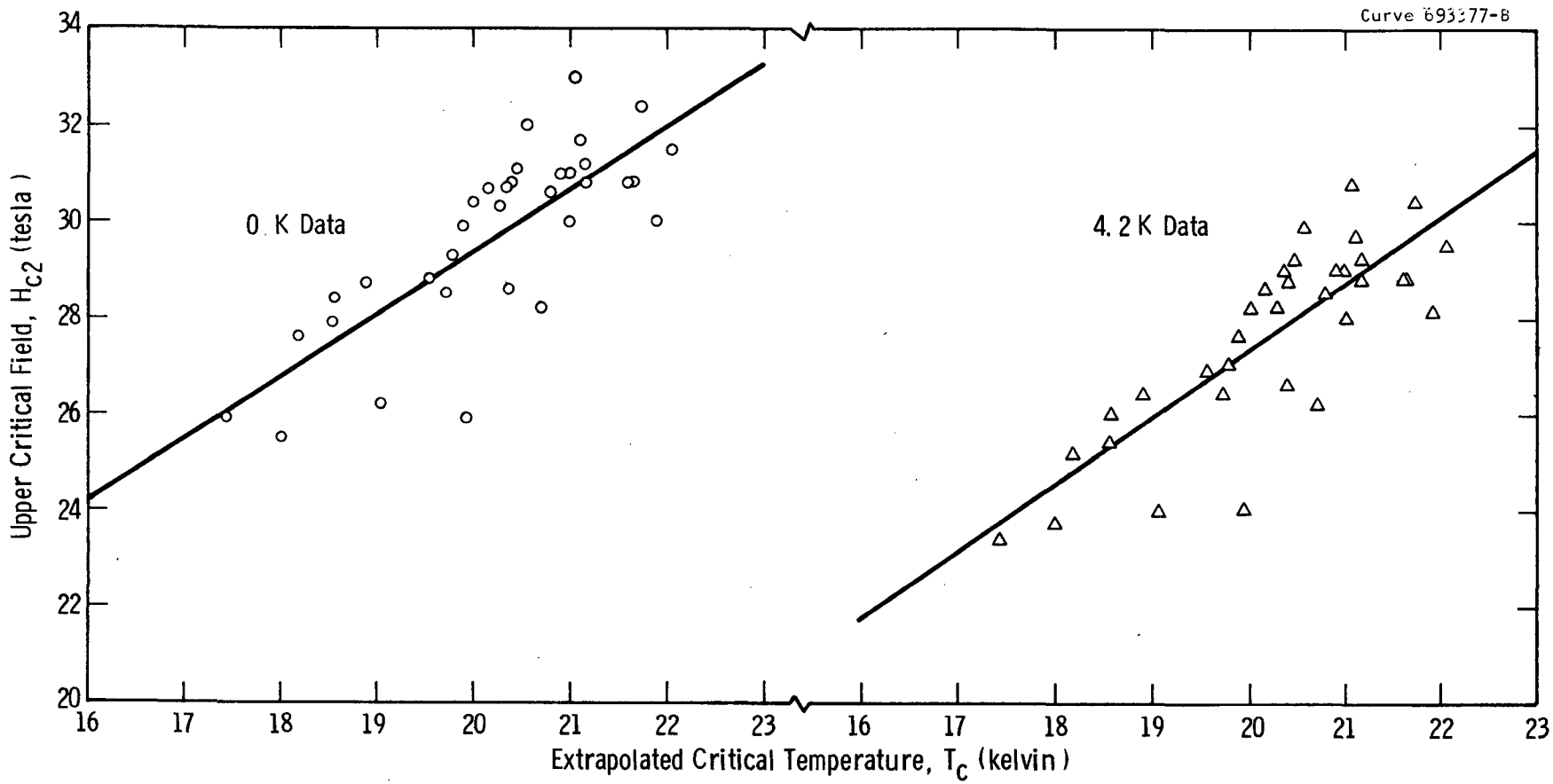

Fig. 14 — Upper critical field, H_{c2} vs. the extrapolated critical temperature, T_c, at 0 and 4.2 kelvin. Straight lines represent least squares fit. Data for Type I and II samples deposited on Hastelloy

lattice and caused by the thermal contraction mismatch between Nb_3Ge and Hastelloy. Indeed, better matched CVD tapes on copper-coated tantalum substrates (Table 9, sample 433) had $dH_{c2}/dT \simeq 2.3$ T/deg. thus attaining the lower limit for sputtered films. Also, early CVD samples deposited on polycrystalline Al_2O_3 had $dH_{c2}/dT \simeq 2.2$ to 2.3 T/deg. although they were probably far from optimum phase uniformity. As seen above internal strains due to the presence of Nb_5Ge_3 inclusions could be the cause of dH_{c2}/dT reduction by ~ 0.1 T/deg. Single-phase CVD deposits on tantalum could attain $dH_{c2}/dT = 2.4$ T/deg. and thus a H_{c2} typical of sputtered samples. Further investigation of the effect of strains on H_{c2} should be conducted.

5.3 Critical-Current Density and Flux Pinning

High-field J_c measurements were performed at 4.2 K by the four-point transport method on copper-coated tape sections $\sim$ 3 cm long and 0.6 cm wide. Measurements were made with the magnetic field perpendicular ($H_\perp$) or parallel ($H_{||}$) to the sample surface using a universal probe, 4 cm in diameter, built by Westinghouse for this program and having a current capability $\geq$ 300 A. The probe size allowed its use in 18 tesla magnets at the National Magnet Laboratory (NML). A smaller < 1.5 cm probe was used in the 1.5 cm dewar bore, 22 tesla NML magnet. In this probe, however, insufficient heat exchange invariably produced thermal runaway of tape samples so that no reliable data could be obtained. Consequently, the upper measuring field limit was 18 tesla.

For flux pinning characterization J's were also determined in the 14 to 20 K range. In this case small samples 1.27 x 0.3 cm were used without any copper stabilization. In all NML transport measurements the voltage of 1 μV across 1 cm of the sample was used to define the transition to normal state.

Lower field J_c measurements up to 6.5 T have been carried out in-house by both, transport and magnetization methods. The purpose was to preselect samples for high-field measurements, to provide quick

feedback information for the CVD experiments and to obtain data for flux pinning characterization.

The high-field properties of Type I samples were summarized in Ref. 21 which is attached to this report as Appendix III. Since that paper did not include J_c (H) graphs covering the high-field range these graphs are reproduced in Figure 15 for NbN, NbC and Nb_5Ge_3-doped samples characterized by transport method. All of the critical-current densities were calculated for the nominal measured thickness values. Subtracting the Ni_3Nb + NiNb diffusion layers would increase the J_c's by approximately 15%. The highest J_c values at 18 tesla were determined for Nb_5Ge_3-doped samples deposited at T_d = 750°C and having relatively low T_c and H_{c2} (see Table 9 and Figure 11). As pointed out in Ref. 22 at a comparable mid-point T_c of ≃ 18 to 19 K the best J_c results were close to the upper limit obtainable for Nb_3Sn. In all of these samples J_c ($H_\perp$) was higher than J_c ($H_{||}$). This indicated that the flux pinning on columnar grain boundaries* made a nonnegligible contribution to the average total pinning force, F_p, in addition to flux pinning on Nb_5Ge_3 impurities. On the other hand these impurities were most effective when intragranular particle sizes were comparable to the coherence length, $\xi_{GL} \cong 50$ Å. Such sizes could be obtained at lower deposition temperatures as shown in Figure 9. Figure 1(c) in Appendix III is a representative micrograph depicting these particles.

Experimental curves of the flux pinning force, $F_p = J_c \times H$ at 4.2 K vs the reduced magnetic field, $h = H/H_{c2}$, are shown in Figure 16, again for samples doped with NbN, NbC and Nb_5Ge_3. Expectedly, highest peak flux pinning forces were obtained for Nb_5Ge_3-doped samples, with $F_{pmax} = 4.5 \times 10^{10}$ newtons/m^3 (4.5×10^9 dynes/cm^3) for sample 277-13, a value typical for best Nb_3Sn tapes fabricated by the diffusion process. Characteristically, all of these samples exhibited peak pinning forces at

---

*For $H_\perp$ the Lorentz force is in the plane of the film while it is normal for $H_{||}$. In the film plane the number density of grain boundaries is greater than along the columns normal to the plane.

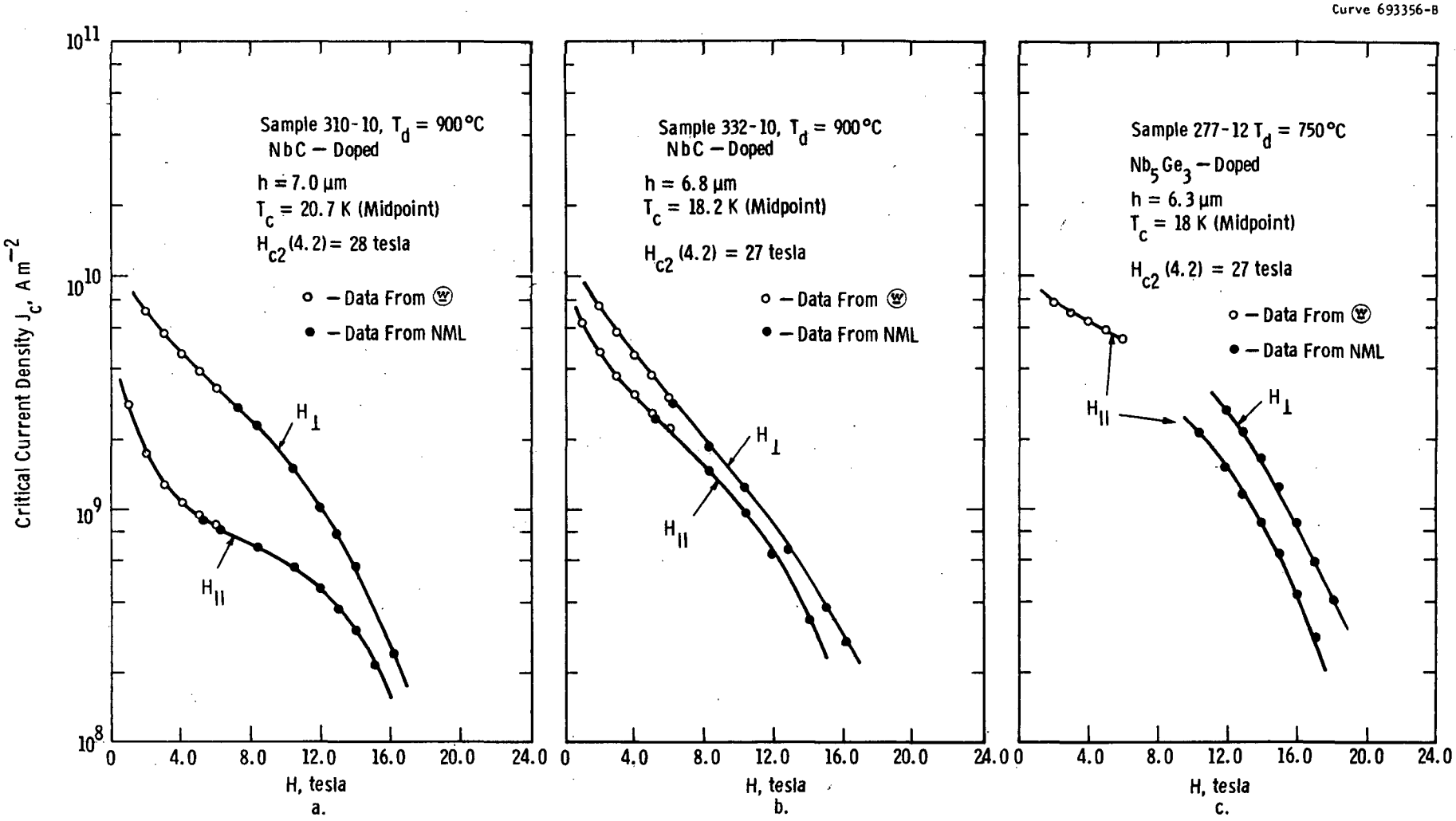

Fig. 15 — Critical current density, J_c, vs. magnetic field intensity, H, at 4.2 K for samples doped with NbN (a), NbC (b) and Nb_5Ge_3 (c)

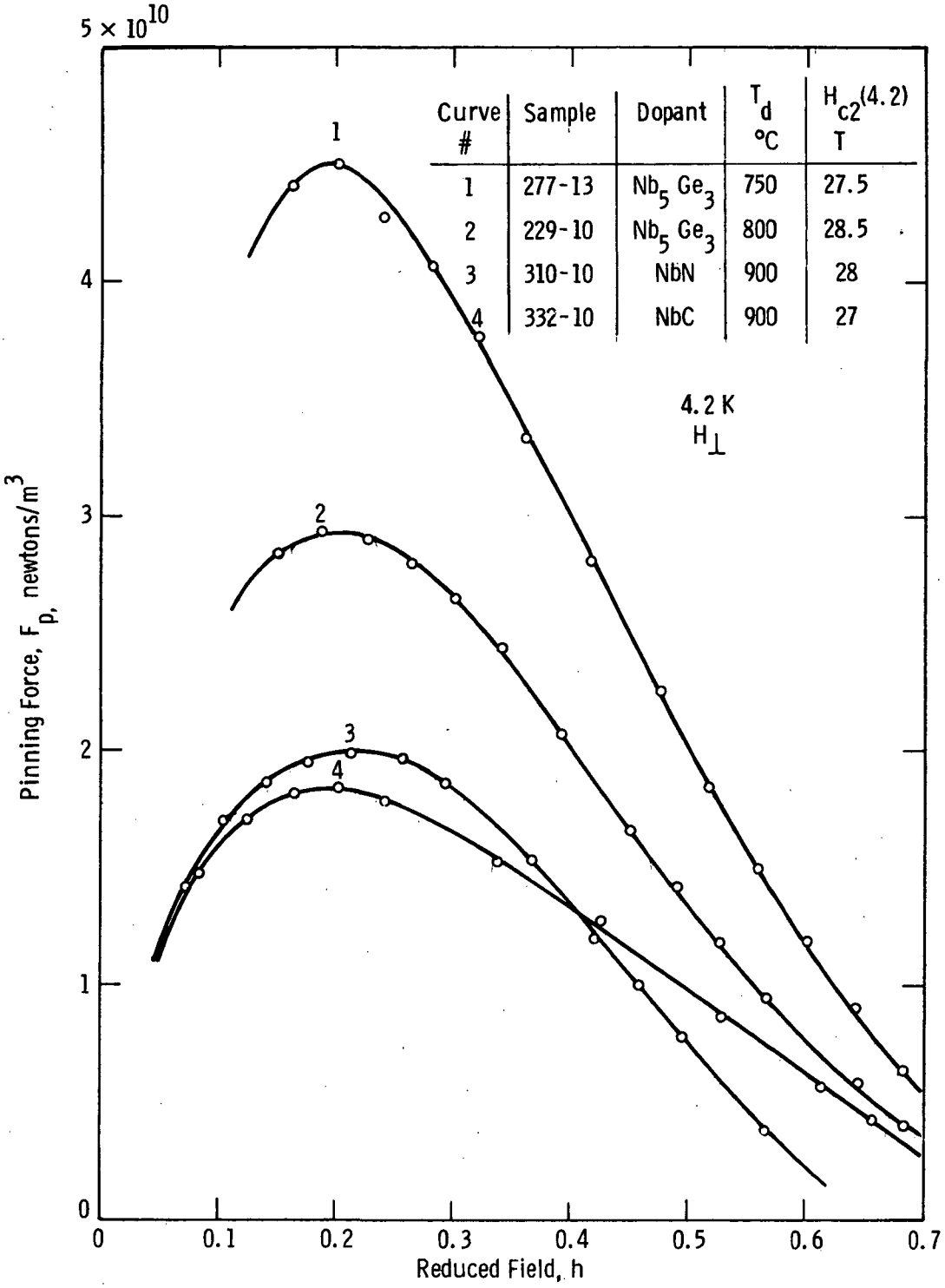

Fig. 16 — Typical flux pinning curves for type I samples doped with various impurities

$h = h_p \simeq 0.2$. In the light of Kramer's flux pinning model[23] one could be thus tempted to conclude that all of these samples had nearly optimum pinning strength. Such a conclusion would be, however, premature since the samples did not obey well the model for $h > h_p$. The scaling law of Fietz and Webb[24] also described the CVD Nb_3Ge only very approximately.[25]

This is illustrated in Figure 17 which shows normalized flux pinning curves at 4.2 K and 10 K for another "optimum" sample, 279-12. The curves clearly did not superpose, contrary to the scaling law. At $h > h_p$ a good fit to Kramer's expression[23] $F_p(h) = K_s h^{1/2} (1 - h)^2$ in which K_s is a constant could, however, be obtained by adjusting h such that the derived H_{c2} values were lower than the experimental data. Lines drawn in Figure 17 correspond to H_{c2} indicated as "fit." At 4.2 K this fit value was typically 15 to 20% lower than H_{c2} determined using the 90% ρ_n criterion and at least 10% lower than that obtained from 10% ρ_n. In the case of sputtered Nb_3Ge the discrepancy was much larger. It is thus probable that all the characterized samples suffered from compositional inhomogeneity. Alternatively, a pin breaking model different from the flux lattice line shear could be operative. This question has not yet been resolved. From a practical point of view it is tempting to believe that improved homogeneity could bring further, dramatic improvement of Nb_3Ge high-field properties. For the present material one should use the scaling laws with caution.

The critical currents and critical-current densities determined for Type II samples at 4.2 K are shown in Figure 18 for the field range from 5 to 18 tesla. Current densities much below 5 tesla could not be measured because of the limitation imposed by the available power supply, $I_{max} \simeq 300$ A. Only magnetization measurements were thus performed between 0.5 and 5 tesla. These were usually consistent with transport measurements. The uncertainty factor was higher, however, than for Type I samples. This was due to greater sample damage occurring when punching discs out of a tape coated on both sides. The J_c values were degraded by a factor of 2 to 3.

Curve 693354-B

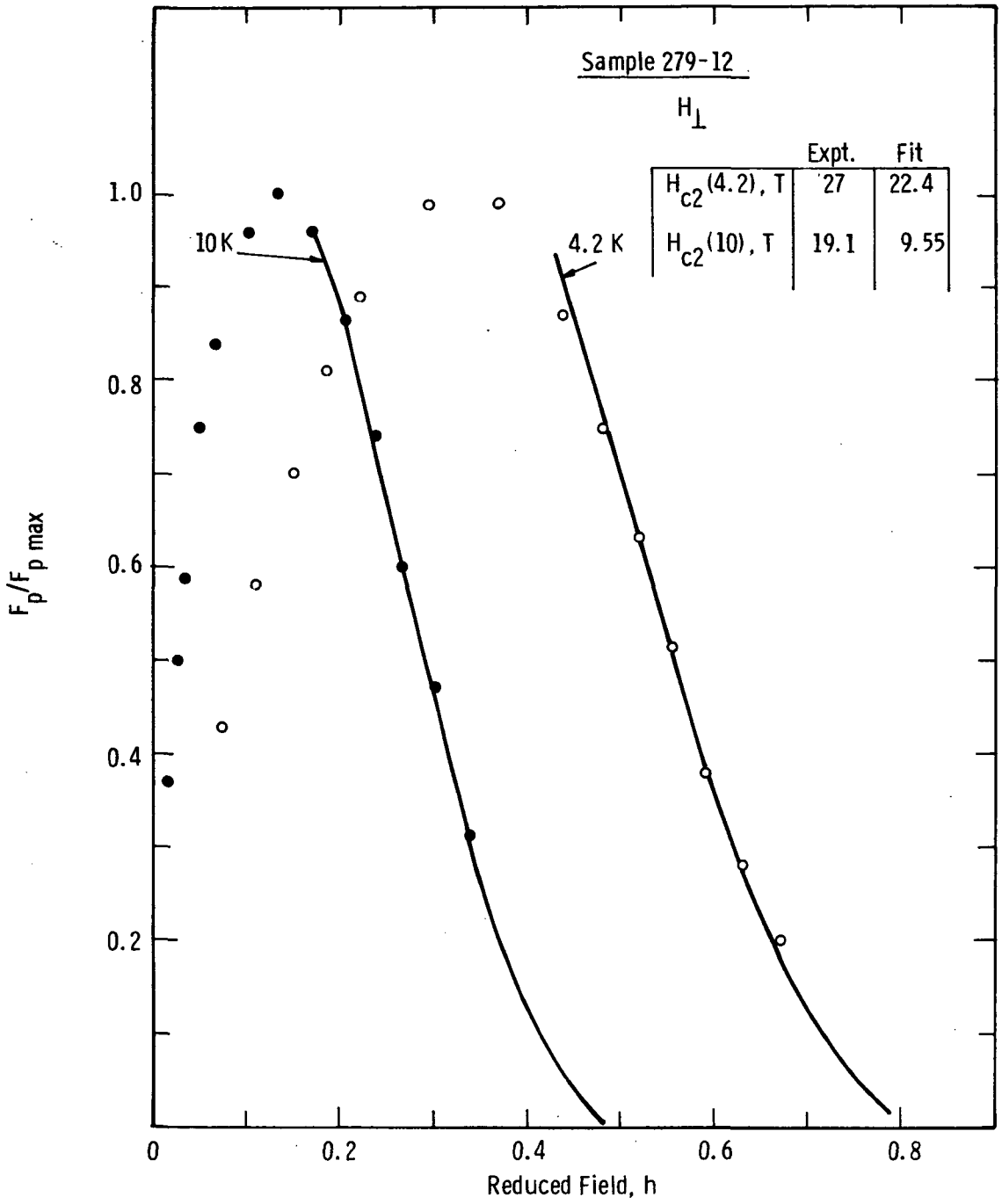

Fig. 17 — Normalized flux pinning curves at two temperatures. Drawn lines represent fit to Kramer's expression[23] for $h > h_p$

Curve 693351-B

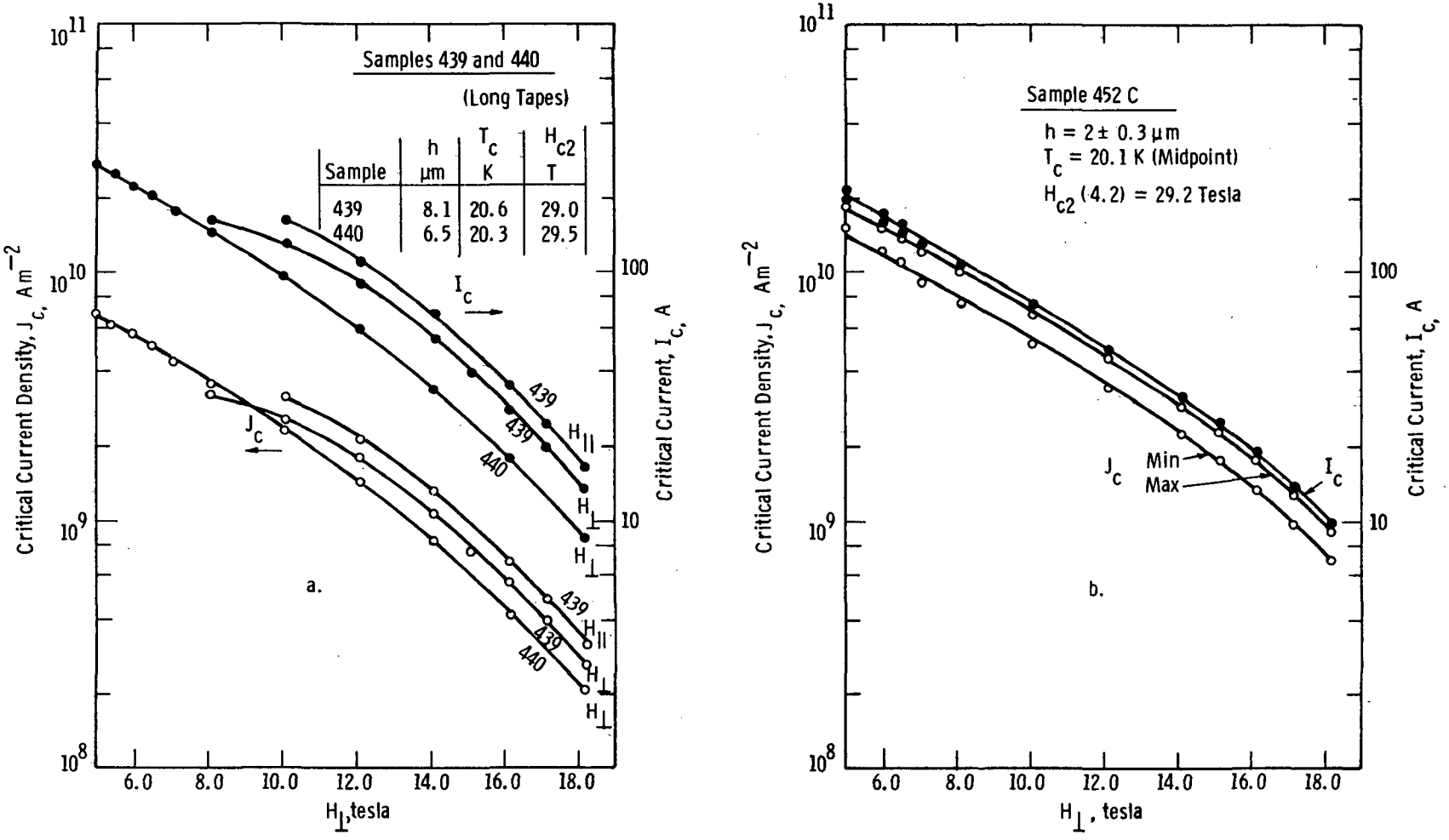

Fig. 18 – Critical current, I_c, and critical current density, J_c, vs magnetic field intensity, H, at 4.2 K. Type II samples of standard (a) and reduced (b) thickness

Comparison of Figures 15 and 18(a) shows that at similar Nb_3Ge thickness of 6 to 8 μm the 18 tesla, 4.2 K critical-current densities of Types I and II samples were comparable and slightly lower than the value $J_c = 5 \times 10^8$ A/m^2 considered as the necessary minimum for building a practical magnet operating at that field and temperature.[21] Interestingly, data of Figure 18(a) and lower field magnetization measurements showed $J_c\ (H_{||}) \geq J_c\ (H_{\perp})$ thus suggesting that the columnar structure of Nb_3Ge deposits was suppressed in Type II samples. No convincing SEM confirmation of an equiaxial microstructure was, however, obtained to date.

Figure 18(b) shows $I_c\ (H_{\perp})$ and $J_c\ (H_{\perp})$ curves for a thinner Type II sample, having a total thickness of 2 ± 0.3 μm (i.e., ∿ 1 μm per side) determined by SEM. This sample, and several similar to it, was deposited over a very short period of time, of the order of 60 sec., in order to obtain a fine grain size, more comparable to that of sputtered specimens. The critical-current density increased dramatically as a result of either an increase in the number density of grain boundaries or relatively larger surface pinning contribution, or both. At 18 tesla, 4.2 K J_c was between 7.5×10^8 and 10×10^8 A/m^{-2} (taking into account the accuracy of thickness determination). It was thus in excess of the required minimum. Extrapolation to 20 tesla gave $J_c = 5 \times 10^8$ A/m^{-2} as a maximum value. This result was still below that for the best sputtered sample ($J_c = 10 \times 10^8$ A/m^{-2} at 21 tesla) but not by much. It indicated convincingly that a CVD material could be optimized to the sputtered sample level by forming fine-grained samples of a required total thickness, e.g., by layering. Layering could also insure a high relative contribution of surface pinning.

Alternatively, fine-grained deposits could perhaps be obtained by direct control of CVD parameters, e.g., by insuring a higher than present nucleation rate.[22]

The flux pinning characteristics of Type II samples were virtually the same as for Type I. Figure 19 shows the pinning force vs h at 4.2 K for one typical tape (#440) and for the thin sample 452C. The

Curve 693355-B

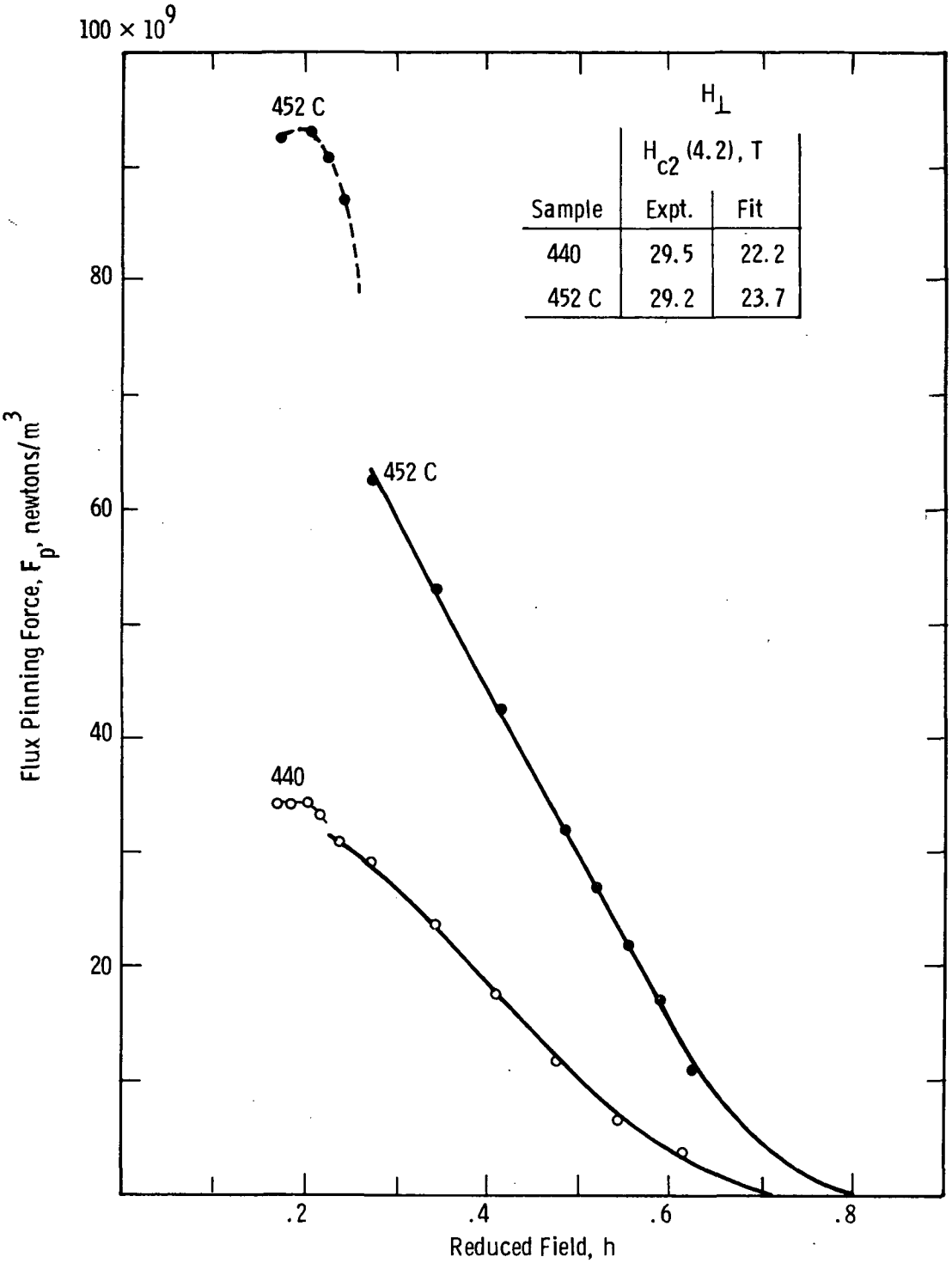

Fig. 19 — Flux pinning force vs reduced field for type II samples. Continuous lines drawn represent fit to Kramer's expression [23] for $h > h_p$

latter curve had a visible kink at $h > h_p$ suggesting the presence of two pinning mechanisms or a pronounced nonuniformity. The peak force was impressive: $F_{pmax} = 93 \times 10^9$ newton/m^3. The fit to theory again produced depressed H_{c2} values indicated in Figure 19.

Figure 20 shows the J_c profile determined for the long tape #440 at 4.2 K and 5 tesla. Comparison with Figure 13 indicates once more that at the beginning of a run tape properties were degraded. Variation of J_c along the tape was relatively slight and gradual indicating a slow drift of deposition parameters (most likely the s = Nb/Ge ratio) with time. The transport J_c's varied within ± 10%. The magnetization measurement produced J_c values lower than the direct, transport measurement due to punched sample damage.

The critical-current densities of samples "layered" by varing s were generally inferior to reference sample properties. Introduction of silane deteriorated the properties even more. Renucleation experiment consisting of pulling the samples cyclically in and out of the deposition zone produced J_c's identical to those of reference samples. Random renucleation did not occur apparently, and the columnar growth continued through all cycles. Microstructures of these samples were not investigated to date.

Clearly the "layering" experiments were too crude to produce meaningful results. The enhanced properties of single thin films such as 452C indicated that this approach has a significant potential.

Curve 693353-B

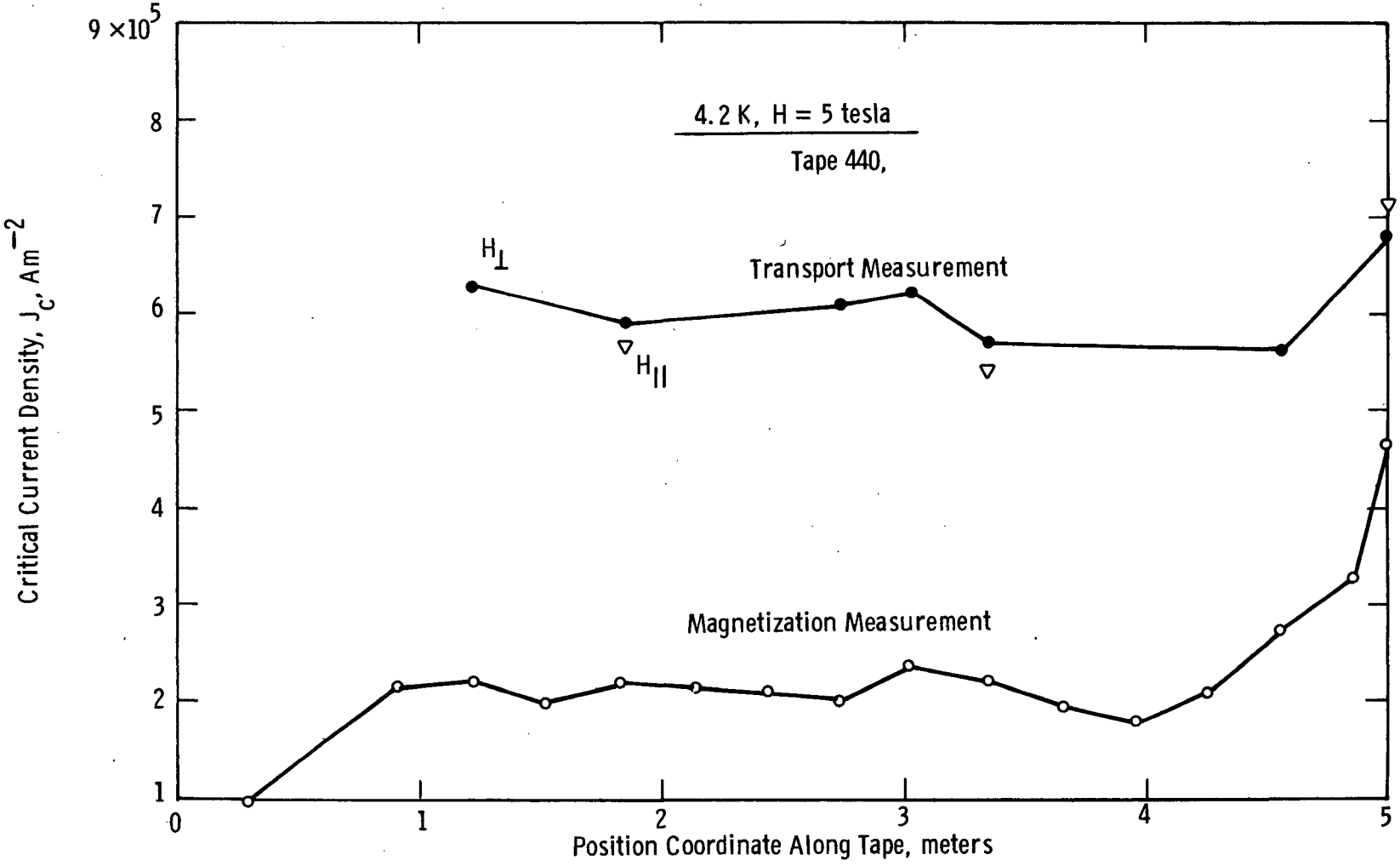

Fig. 20 — Critical current density profile along tape #440

6. DISCUSSION

6.1 Preamble

The preceding section describes what was the first relatively detailed study of high-field superconducting properties of Nb_3Ge. Other "firsts" were the successful attempts to fabricate lengths of Nb_3Ge tape conductors and to achieve high levels of flux pinning on second-phase impurities. It is not surprising, therefore, that this program left many significant questions unanswered, and problems unsolved. While some of these problems are or, hopefully, will be studied within independent projects it is appropriate to discuss here the major directions of future work aimed at developing Nb_3Ge tape conductors for high-field magnet applications. While this goal may appear restrictive it should be obvious that progress in tape conductors will form a necessary foundation for an ultimate development of filamentary Nb_3Ge.

6.2 Fabrication

With regard to tape fabrication it is clear that the present CVD process needs further improvement in uniformity control, both in coating geometry and in time, to produce long conductors having well defined, constant properties. Capability of producing layered deposits should be insured by modifying the CVD system. A system modification allowing the use of ohmic heating of substrates with the aim to improve productivity would also be desirable. Quality assurance procedures have to be established and implemented. Cladding of long conductors with high-resistance-ratio copper must be developed and test solenoids fabricated to characterize the composite conductors in realistic environments prior to building a prototype magnet. All of the above tasks are relatively trivial, well within the present technological capability of Westinghouse

and other qualified groups. It is essentially a problem of adequate funds and time, but not a long time at that. A preliminary description of that type of fabrication program was submitted to NASA-Lewis in November of 1976.[26]

A broader question should be asked, however. Is CVD really the preferred approach to Nb_3Ge conductor fabrication? In 1976 this group had serious doubts about it, thinking that physical vapor deposition (PVD) would offer a better road to success, this being a cleaner and easier to control process possibly resulting in finer microstructures.[6] Perhaps that holds true, but after another year and a half CVD still leads both in process development and superconducting properties achieved on practical, metallic substrates. In the case of low energy and magnetron sputtering the properties of Nb_3Ge on sapphire substrates could not be reproduced when depositing on metallic surfaces.[21] A better understanding of the high-T_c A15 phase nucleation and stabilization is a prerequisite for progress in sputtered Nb_3Ge. Such improved understanding would automatically benefit CVD as well.

Much more study and data is needed on the electron-beam deposition of Nb_3Ge. One very promising and important discovery was that of "polycrystalline epitaxy" on a metallic A15 Nb_3Ir surface.[10] A study of high-field properties of E-beam deposited Nb_3Ge is highly desirable and could be carried out taking advantage of the capability of Stanford University with their unique E-beam machine suitable for preparing some lengths of Nb_3Ge tape. It is, however, difficult to assume a priori that the results of such a study will surpass those of CVD work. By the end of 1977 the CVD fabrication of Nb_3Ge appears to represent the safest bet.

6.3 Mechanical Properties, Load Tolerance

For Nb_3Ge this is still a virgin territory. One would expect the material's properties to be analogous to other A15's, particularly Nb_3Sn. The type of substrate used and the resulting prestressing of the

superconductor should determine the mechanical load tolerance. That tolerance must be tested experimentally prior to the final substrate selection. A test study in collaboration with the National Bureau of Standards, Cryogenics Division was initiated recently under an independent program* and it should permit an eventual optimization of tape conductor mechanical properties. Until test results became available the rejection of present Hastelloy B substrate will be premature. If copper-clad tantalum or niobium were used it will be advantageous to form an asymmetrical tape, with the superconductor on one side of the substrate. Upon bending on a mandrel the superconductor will then be subject to only one, least deleterious type of applied stress, either compressive or tensile, so that the intrinsic strain could be minimized. As in the case of fabrication processes the problems related to mechanical properties are relatively well defined. Approaches to further development work are clear.

6.4 Superconducting Properties Vs Microstructure and Phase Homogeneity

For high-field applications the maximization of the critical temperature of Nb_3Ge is of concern primarily as a means to maximize H_{c2}. The present level of T_c in Nb_3Ge tapes (20 to 21 K) is less than maximum as a result of trade-offs necessary to insure high critical current densities and the conductor practicality. The presence of Nb_5Ge_3 second-phase, and other impurities, e.g., unreduced chlorides in tapes deposited at relatively low temperatures depresses T_c by 0.5 to 1 K. The substrate mismatch strains possibly reduce T_c by another 0.5 to 1 K. Ideally, one would like to deposit fine-grained, unstrained, single-phase deposits at higher temperatures, 900 to 950°C. That might be possible by layering the films. The layering approach should be pursued vigorously, in analogy to the E-beam work on layered Nb_3Sn films.[27] Results of Section 5.3 clearly show the significant improvement in the high-field critical-current density that results from reducing the layer thickness

---

*Air Force Office of Scientific Research Contract No. F44620-74-C-0042.

and, presumably, the grain size. An alternative approach could be to inhibit grain growth by suitable impurity, third element substitution or deposition process modification. Layering, of course, will not reduce the effects of strain upon T_c, H_{c2} and J_c. These effects should be studied in conjunction with the investigation of mechanical properties. For H_{c2} and T_c they do not appear dramatic in the light of data presented in Section 5.2.

The problem that stands out as a result of the present study is the flux pinning mechanism at high fields. This problem is common to CVD and sputtered Nb_3Ge and it would be interesting to see whether it is shared by E-beam evaporated films, especially the "epitaxial" ones.

The flux lattice line (FLL) shear model should be applicable to all strongly pinned, hard superconductors. One is thus tempted to believe that the strongly depressed H_{c2} values necessary to fit the FLL model suggest a major A15 phase inhomogeneity. There is, however, no X-ray evidence of it. Why? If, on the other hand, the A15 phase is homogeneous, what makes the pinning mechanism in Nb_3Ge different? The strength of pins and their number density have apparently no effect here as witnessed by the data of Section 5.3. Were the flux pinning force dependent upon field in the same way as in other superconductors then the high-field J_c's would be very much higher for present T_c and H_{c2} values. From the point of view of high-field application of Nb_3Ge it is important, therefore, to solve the above problem.

7. CONCLUSIONS

- The objective of this study have been attained and in certain areas surpassed.
- The study confirmed that chemical vapor deposited Nb_3Ge has potential for application in high-field magnets.
- The study has shown that present Nb_3Ge tape conductors can be used at 4.2 K in fields up to 16 to 18 tesla.
- Flux pinning on second-phase particles was successfully used to enhance critical-current densities.
- Possibility of improved Nb_3Ge performance up to at least 20 tesla was demonstrated.
- Tape conductors up to 10 meters long were demonstrated.
- Problems requiring further study were identified.

8. RECOMMENDATIONS

Future research on Nb_3Ge for high-field applications should include several parallel studies on topics listed below in order of priority:

1. Mechanism of flux pinning and pin breaking in high magnetic fields in relation to A15 phase homogeneity and stability.
2. Correlation of microstructure with flux pinning strength, effect of layering on critical-current density, grain growth inhibition by additives or deposition control.
3. Effect of strain upon critical temperature, upper critical field and critical-current density.

The next steps in the development of chemical vapor deposited Nb_3Ge tape conductors for magnets should be as follows:

1. Develop fabrication methods for long composite, i.e., copper-clad Nb_3Ge tapes.
2. Test mechanical load tolerance and select optimum substrate tape.
3. Develop, fabricate and test experimental Nb_3Ge solenoids.
4. Establish and implement quality assurance procedures.
5. Build a prototype magnet.

9. ACKNOWLEDGMENTS

The use of the National Magnet Laboratory facilities is gratefully acknowledged. Special thanks are due to Mr. Larry G. Rubin of NML for his hospitality and also for the friendly and most accommodating help in solving last-minute technical problems.

10. REFERENCES

1. J. R. Gavaler, "Superconductivity in Nb-Ge Films Above 22 K," Appl. Phys. Lett. 23, 8, 480 (1973).

2. S. Foner, E. J. McNiff, Jr., J. R. Gavaler and M. A. Janocko, "Upper Critical Fields of Nb_3Ge Thin Film Superconductors," Phys. Lett. 47A, 6, 485 (1974).

3. A. I. Braginski and G. W. Roland, "Chemical Vapor Deposition of Superconducting Nb_3Ge Having High-Transition Temperatures," Appl. Phys. Lett. 25, 12, 762 (1974).

4. L. R. Newkirk, F. A. Valencia, A. L. Giorgi, E. G. Szklarz and T. C. Wallace, "Bulk Superconductivity Above 20 K in Nb_3Ge," IEEE Trans. MAG-11, 2, 221 (1975).

5. A. I. Braginski, G. W. Roland, M. R. Daniel, A. T. Santhanam and M. A. Janocko, "An Improved Superconductor for Transmission Line Applications, Phase II," U. S. ERDA Report CONS-2522, June 1976.

6. A. I. Braginski, J. R. Gavaler, G. W. Roland, M. R. Daniel, M. A. Janocko and A. T. Santhanam, "Progress Toward a Practical Nb_3Ge Conductor," IEEE Trans. MAG-13, 300 (1977).

7. A. I. Braginski, G. W. Roland, M. R. Daniel, A. T. Santhanam and K. W. Guardipee, "Impurity Doping of CVD Nb_3Ge and Its Effect on Critical-Current Density," to appear in J. Appl. Phys. (Feb. 1978).

8. G. W. Roland and A. I. Braginski, "Chemical Vapor Deposition of Nb_3Ge," Adv. Cryo. Eng. 22, 347 (1977).

9. A. I. Braginski, G. W. Roland and M. R. Daniel, "Preparation of Nb_3Ge by Chemical Vapor Deposition," Appl. Polymer Symp. No. 29, 93 (1976).

10. A. H. Dayem, T. H. Geballe, R. B. Zubeck, A. B. Hallak and G. W. Hull, Jr., "Epitaxial Growth of High-T_c Superconducting Nb_3Ge on Nb_3Ir," Appl. Phys. Lett. 30, 541 (1977).

11. L. R. Newkirk (Los Alamos Scientific Laboratory), private communication.

12. (a) Y. S. Toloukian, R. W. Powell, C. Y. Ho, and P. G. Klemens, "Thermal Conductivity - Metallic Elements and Alloys, Vol. 1," IFI/Plenum, NY, 1970. (b) Y. S. Toloukian, R. K. Kirby, R. E. Taylor and P. D. Desai, "Thermophysical Properties of Matter, Vol. 12 - Thermal Expansion of Metallic Elements and Alloys," IFI/Plenum, NY, 1975.

13. C. J. Smithells, "Metals Reference Book," 4th Edition, Plenum, NY 1967.

14. F. R. Schwartzberg, "Cryogenic Materials Data Handbook," Report ML-TDR-64-280, Air Force Materials Laboratory, August 1964.

15. E. Veleckis, "Thermodynamic Properties of the Systems: Nb-H, V-H and Ta-H," Ph.D. Thesis, Illinois Inst. of Technology, January 1960 (cited in "Metal Hydrides" by W. M. Mueller, J. P. Blackledge and G. G. Libowitz, Acad. Press 1968.

16. J. W. Ekin, "Fatigue and Stress Effect in NbTi and Nb_3Sn Multifilamentary Superconductors," Paper CA-1, 1977 CEC-ICMC Conf., Boulder, Colorado.

17. G. Rupp, "Improvement of the Critical Current of Multifilamentary Nb_3Sn Conductors Under Tensile Stress," IEEE Trans. MAG-13, 1565 (1977).

18. G. W. Hull and L. R. Newkirk, "Thermal Expansivity of Nb_3Ge," J. Low Temp. Phys. (in press, 1977).

19. A. T. Santhanam, A. I. Braginski, G. W. Roland and M. R. Daniel, "Correlation of Microstructure and Critical-Current Density in Nb_3Ge," (to be submitted for publication).

20. E. Helfand and N. R. Werthamer, "Temperature and Purity Dependence of the Superconducting Critical Field, H_{c2}, II," Phys. Rev. 147, 288 (1966).

21. M. R. Daniel, A. I. Braginski, G. W. Roland, J. R. Gavaler and A. T. Santhanam, "Nb_3Ge as a Potential Candidate Material for 15 to 25 T Magnets," CEC-ICMC Conf., Boulder, CO, August 1977, Paper KA-7.

22. R. A. Holzl, "Grain Refinement by Thermochemical Means," Proc. 6th Int. Conf. on CVD, 77-5, 107 (1977).

23. E. J. Kramer, "Scaling Laws for Flux Pinning in Hard Superconductors," J. Appl. Phys. 44, 1360 (1973).

24. W. A. Fietz and W. W. Webb, "Hysteresis in Superconducting Alloys," Phys. Rev. 178, 657 (1969).

25. M. R. Daniel, A. I. Braginski, G. W. Roland, J. R. Gavaler, R. J. Bartlett and L. R. Newkirk, "Temperature Dependence of J_c in Superconducting Nb_3Ge," J. Appl. Phys. 48, 1293 (1977).

26. Program for the Development and Magnet Test of Nb_3Ge Tape Conductors for Very High-Field Generation, Westinghouse Preliminary Program Description 6M729 (November 1976).

27. R. E. Howard, M. R. Beasley, T. H. Geballe, C. N. King, R. H. Hammond, R. H. Norton, J. R. Salem and R. B. Zubeck, "Electrical Properties of Multilayered Nb_3Sn Superconducting Power Line Conductors," IEEE Trans. MAG-13, 138 (1977).

11. PARTICIPATING WESTINGHOUSE PERSONNEL

1. A. I. Braginski - Principal Investigator, CVD development, high-field characterization and interpretation.
2. M. R. Daniel - High-field characterization and interpretation.
3. A. L. Foley - Mechanical parts design and CVD assistance.
4. J. R. Gavaler - Comparative sputtering experiments, high-field characterization.
5. R. C. Kuznicki - X-ray diffractometer.
6. T. A. Manion - X-ray diffractometer.
7. M. T. Miller - CVD operation.
8. P. A. Piotrowski - CVD operation.
9. H. C. Pohl - High-field (J_c) measurements.
10. G. W. Roland - Co-Principal Investigator, CVD development, phase studies.
11. A. T. Santhanam - Microstructure study, TEM.
12. J. J. Schreurs - Auger Spectroscopy.
13. G. G. Sweeney - SIMS Analysis.
14. R. Wilmer - T_c measurements.
15. P. Yuzawich - TEM sample preparation.

Page Intentionally Left Blank

APPENDIX I

STATEMENT OF WORK
(NAS3-20233)

A. Task 1 - Optimization of Deposition Parameters

Using chemical vapor deposition (CVD) methods, the contractor shall optimize deposition parameters of Nb_3Ge on substrates of Hastelloy and/or stainless steel at substrate temperatures of 900 ± 10°C. The parameters to be optimized shall be at least those of reactant rates, delivery rates, and dilution; ± 10% thickness uniformity and ± 10% $J_c(H, T)$ uniformity over 1 foot lengths are desired.

At the completion of this task the contractor shall deliver to the NASA Project Manager a one (1) foot long state-of-the-art high T_c Nb_3Ge tape. This tape shall be the highest J_c, H_c, and T_c over longest length.

The contractor shall characterize the substrate material, including identification of phase, composition, microstructure, and thermal expansion.

B. Task II - Determination of Effects of Deposition Temperatures

The contractor shall determine the effects of deposition temperature on $J_c(H, T)$, within the temperature range of 700 to 900°C. The contractor shall deliver to the NASA Project Manager a one (1) foot section of high T_c Nb_3Ge tape which is optimized to the highest J_c, H_c, and T_c.

The contractor shall characterize the substrate material, including identification of phase, composition, microstructure, and thermal expansion.

Page Intentionally Left Blank

APPENDIX II

CHEMICAL VAPOR DEPOSITION AT THE TERMINATION OF ERDA'S PROGRAM

1. Scope

The purpose of this appendix is to summarize the information on the fabrication process which may be helpful in discussing the data not reported in earlier publications.[1,2] Furthermore, the results leading to a moving tape CVD reactor design are presented and the reactor described.

2. Deposition of Single Elements and Parameters of Co-Deposition

Work on deposition of elemental Nb and Ge was performed prior to Phase II under a different program,* and was already reported.[1] It is, however, useful to present data which served as a basis for selecting the parameters used in the present program for Nb and Ge co-deposition by reducing a generated mixture of $NbCl_4$ and $GeCl_2$ vapors with hydrogen. The single element data are limited to low values of $r \leq 15$, where r is the molar ratio of hydrogen to chloride, $NbCl_4$ or $GeCl_2$, in the gas phase delivered to the reaction tube. As a result of the discovery of the tetragonal T2 phase,[2] much higher r values, 80 to 330, were subsequently used to prevent the T2 occurrence. Nevertheless, the single element data provided useful qualitative guidelines for the interpretation of co-deposition results. Measured were: (1) the total reaction yield or efficiency, Y, defined as the ratio of the element mass deposited to the element mass delivered in the form of the chloride, and (2) the longitudinal profile of growth rate in the deposition tube. The experiments have been performed using quartz substrate tubes of $\sim$ 2.5 cm ID and

---

*Contract No. AFOSR-F44620-74-C-0042.

various length. Helium was used as inert carrier gas. The total gas phase velocity, v, was considered as one of the parameters of the process.

Figure 1 shows Y(r) for niobium at three temperatures. Yield increases with T_d and r (and eventually saturates at high r values). Analogous results were obtained for Ge.

Figure 2 compares Y(r) for Nb and Ge at T_d = 800°C. The efficiency of germanium chloride reduction was found to be higher than in the case of $NbCl_4$ in the whole temperature range investigated (750 to 950°C). Hence, a preferential deposition of germanium, and the resulting preferential depletion of gas phase, could be expected in the case of co-deposition.

Figure 3 shows Ge growth rate profiles as a function of r. With increasing r the reaction rate increased, the gas phase depleted more, and consequently the profiles show a pronounced peak even before the temperature reaches the plateau (T_d = 800°C) on the inlet side of the tube. Analogous results were obtained for Nb. The use of low r to obtain flat film thickness profiles thus appeared desirable.

Figure 4 shows Ge growth rate profiles as function of total gas velocity at r = 10. Higher gas velocities at constant $GeCl_2$ delivery were obtained by increasing the delivery rate of carrier gas. Hence, changes in v are associated with changes in vapor phase dilution by the inert carrier. Increasing v resulted in flattened rate profiles. This was interpreted as the result of finite residence time required for the reaction, rather than the effect of dilution. The effect of dilution was separately studied by setting v and r constant at T_d = 800°C, and varying the delivery rate from 0.02 to 0.3 mole/hour. The yields were found to be almost independent of the delivery within the above limits. The results for Nb were again analogous. Hence, the Y(r, T_d, v) data provided directly usable information for scaling and predicting growth rates.

The results shown above formed a base for assuming standard conditions used in early co-deposition experiments.[1] Assumed were: $T_d \simeq 900°C$, r = 10, v = 500 cm/sec. The chloride delivery level was

0.15 mole/hour for thick deposits and 0.03 mole/hour for thin layers. In these conditions it was indeed possible to obtain relatively flat growth rate profiles so that deposition of stationary substrate tapes, up to 0.3 m long appeared possible.[1] However, once much higher r values were implemented (to eliminate the T2 phase) with other deposition parameters unchanged the rate profiles became much steeper. From that point on the program centered on studying the x-profiles of the tape properties.* No attempts were made to flatten the profiles by increasing v_x significantly above 500 cm/sec.

The gas delivery rates were already pretty high: $\sim$ 20 ℓ/min for the H_2 + He mixture. Also, v could not be increased significantly without a transition from laminar to turbulent flow regime. Consequently, the gas velocity, and the chloride delivery rates were maintained on the previous level. Varied were: T_d, r and s.**

3. The CVD Gas Phase: Nb/Ge Ratio

An earlier publication[1] described the CVD reactor and the manner in which the gas phase Nb/Ge molar ratio, s, was controlled by the Cl_2 gas flows through the Nb and Ge chlorination beds. It was evident, however, that the s value for the gas phase at the deposition zone was somewhat different because of the formation of deposits in the reactor mixing zone. Consequently, the deposits in the reactor mixers were analyzed and some idea of the magnitude of the correction required for s was obtained.

Two types of deposits occurred in the mixing zone: (1) a black granular material and (2) a metallic coating. Chemical analyses of the black deposit gave an average value of 42.2 wt. % Nb, 9.4 wt. % Ge, 48.4 wt. % Cl. This composition recalculates to (Nb, Ge)$Cl_{2.3}$, consistent with the existence of a black niobium chloride phase having $NbCl_{3-x}$

---

*x is the position coordinate along the stationary tape.

**$s = NbCl_4/GeCl_2$.

composition. It is quite probable, however, that a mixture of chloride phases was present. The metallic phase was chloride-deficient and very variable in composition. In all cases, the black chloride-rich material was predominant, e.g., for a typical series of runs (total running time 120 minutes) at deposition temperature, T_d = 900°C, the total accumulated black deposit in the mixing zone was 15.4 grams. The metallic deposit amounted to less than a gram.

Material lost in the mixing zone has two effects: (1) the total amount of Nb and Ge delivered to the deposition zone is reduced, and (2) the value of s at the deposition zone is changed. For the series of runs described above, the amount of Nb and Ge delivered was reduced by 26% and 36% respectively. Because of the larger reduction in Ge, the s value correspondingly increased 14%. For economic reasons the loss of material is a more important problem than a change in s value. Therefore, in a commercial process, a system using $NbCl_5$ and $GeCl_4$ as sources of Nb and Ge would offer advantages since gas mixing can then be done at low temperature where mixing-zone deposits do not form.

4. The Nb-Ge Growth Rates and Yield

The deposited tapes have been cut into ∿ 5 cm sections, and the growth rate, h_t (in μm/hour) determined from each section deposit weight, assuming a standard substrate weight. This way the growth or deposition rate profiles h_t (x), where x is the position coordinate in the deposition zone, could be obtained. The value x = 0 was assigned to a point where the gas temperature reached a constant level, T_d. For $x > 0$, $T = T_d$ while for $x < 0$, $T < T_d$.

Table 1 presents $h_t(x)$ data obtained at T_d = 900°C, in the constant temperature deposition zone, for various r and s values where s is the molar ratio Nb/Ge in the generated chloride mixture (uncorrected for losses in the mixing zone). Table 2 gives $h_t(x)$ data for various T_d and extreme s values at a constant r = 200.

Table 1 - Growth Rate Profiles h_t (x) in μm/hour for Various r and s Values, T_d = 900°C.

Run No.	r	s	x = 0 cm	x = 10 cm	x = 20 cm	x = 30 cm	x = 40 cm
211	80	2.5	72	53	37	31	23
206		3.1	75	52	35	26	17
207		3.6	67	49	28	26	19
208		4.2	75	56	42	36	21
209		5.0	65	50	26	25	21
212		8.3	66	51	27	24	19
195	200	2.5	76	42	23	13	9
184		3.1	53	33	18	19	14
181		3.6	74	44	30	23	13
202		4.2	61	45	33	23	19
182		6.3	63	38	27	25	14
183		8.3	62	42	27	22	18
196	330	2.5	68	24	28	19	5
193		3.1	108	45	17	11	7
192		3.6	51	39	24	17	8
188		4.2	41	21	11	11	2
189		5.0	49	35	23	17	7
191		8.3	36	33	18	9	11

Table 2 - Growth Rate Profiles h_t (x) in μm/hour for Various T_d and s Values, r = 200.

Run No.	T_d K	s	x = 0 cm	x = 10 cm	x = 20 cm	x = 30 cm	x = 40 cm
275	750	3.1	64	46	43	34	29
273		6.3	44	42	29	36	23
231	800	3.1	76	45	29	24	21
227		6.3	63	52	30	29	21
375	850	3.6	37	45	27	22	24
372		6.3	65	45	25	23	16
184	900	3.1	53	33	18	19	14
182		6.3	63	38	27	25	14
259	950	2.5	63	35	12	4	3
253		6.3	68	39	28	8	3
265	1000	3.1	67	47	20	5	≈0
261		6.3	59	42	15	11	7

Both tables show that the growth rates decrease along the deposition zone, i.e., with increasing x. This is a result of the gas phase depletion, and generation of HCl in the chloride reduction reaction with hydrogen.[1] At high deposition temperatures, and higher r values, the reduction efficiency of both elements is high and the depletion more pronounced. Hence, $h_t(x)$ decreases more steeply with increasing x. However, in the whole range of T_d, from 750 to 1000°C, the rates are comparable, 40 to 80 μm/hour at x = 0, if r is sufficiently high, i.e., in the range shown. For low $r \lesssim 10$, rates are prohibitively low at 750°C due to low reduction efficiency. Since low r values have been originally used for Nb-Ge deposition,[1] temperatures below T_d = 800 to 850°C were considered impractical. The need for high r to prevent the formation of the T2 phase automatically extended the temperature range down to 750°C. However, the presence of Nb chloride lines ($NbCl_{2.66}$) was observed in X-ray diffraction patterns of some deposits grown at 750°C thus indicating that the reduction was not complete.

Figures 5 and 6 show the $h_t(x)$ profiles over the whole deposition zone, including the inlet zone ($x < 0$) where $T < T_d$. In addition to illustrating the stronger gas phase depletion effect at higher T_d and/or r, the graphs show that deposition occurs at a high or peak rate in the inlet zone ($x < 0$). For low s, set such that the tetragonal Nb_5Ge_3 (σ phase) deposits at x = 0, the h_t peaks at $x \leq 0$ are much higher than in the case of A15 and shifted to lower x (lower temperature). This suggests that the free energy of formation of the tetragonal phase is lower than that of A15, and also that the gas phase is preferentially depleted in Ge already at x = 0. A larger fraction of the deposit is thus lost in the inlet zone. In consequence, for given T_d and r the rates at $x > 0$ are similar for both, σ and A15 deposits.

Table 3 gives effective yield data for the investigated range of T_d, r and s. The effective yield, Y_{eff}, is defined as the ratio of the mass of solid deposited on the 1.27 cm wide tape substrate in the constant temperature zone (x = 0 to 40 cm) to the mass of metal converted into chlorides. The values of Y_{eff} are uniformly low, 7 to 15%, due to:

Table 3 - Yield of Solid Deposit on Substrate in the Constant Temperature Zone, Y_{eff}, for Various Values of T_d, r, and s

Run No.	T_d °C	m	s	Y_{eff} %
275	750	200	3.1	15.9
273			6.3	13.6
231	800	200	3.1	12.8
227			6.3	15.3
375	850	200	3.6	10.4
372			6.3	12.8
211	900	80	2.5	14.9
212			8.3	15.4
195		200	2.5	10.4
183			8.3	14.1
196		330	2.5	9.0
191			8.3	8.3
259	950	200	2.5	7.2
253			6.3	10.0
265	1000	200	3.1	9.6
261			6.3	10.1

(1) losses in the mixing zone (Section 3), (2) deposition in the inlet zone ($x < 0$), (3) deposition on the walls of the reactor tube in the deposition zone. The effective yield decreases slightly with increasing T_d and r, due to stronger depletion in the inlet zone which is also responsible for the fact that in most cases Y_{eff} (A15) > Y_{eff} (σ). The total yield of the reduction reaction at high r is very high, approaching 100%, when taking into account the mixing zone loss.

The level of h_t and Y_{eff} appears acceptable for a fabrication process, although higher values of h_t, of the order of 100 to 200 μm/hour would be preferable from the economical point of view. However, if (2) and (3) could be prevented, then at comparable h_t and Y_{eff} a much flatter $h_t(x)$ profile could be obtained due to reduced depletion of the gas phase. This possibility is discussed in Section 6.

5. Substrate Materials and Deposition Geometry

During the course of the work, the Nb-Ge films have been deposited on various substrate materials. The typical substrate material was a Ni-base stainless steel, Hastelloy B which was in the form of a tape 1.27 cm wide and 50 μm thick. Additional substrate materials were Cu, Nb, polycrystalline alumina, single-crystal sapphire, Type 303 stainless steel, and Cu-clad Nitronic stainless steel. No adhesion problems were encountered in the case of Cu or Cu-clad materials, polycrystalline alumina, or sapphire. Deposits on Nb required that the Nb be carefully cleaned by etching (for oxide removal) with a solution composed of 50 ml HNO_3, 50 ml HF, 10 ml H_2O_2 for the deposit to adhere. Unfortunately, this was established by the end of the program. Deposits on Type 303 stainless steel were easily spalled away from the substrate due to strain caused by thermal expansion mismatch.

For most of the studies, the substrate material was held on a flat quartz sample holder designed to be positioned along the deposition zone of the CVD reactor. In this geometry, therefore, deposition occurred only on one side of the substrate, that surface exposed to the gas phase

in the CVD reactor tube. As a result the tape was always deformed with the top (Nb_3Ge) side convex. A substrate uniformly coated by Nb_3Ge on both sides is necessary to fabricate a flat, undeformed conductor.

6. Moving-Tape CVD Reactor

In Section 2 it was shown that, because of reactor design and the nature of the CVD gas-phase reaction, it was not possible to achieve uniform Nb-Ge deposit properties in the stationary substrate reactor. This was especially true after increasing r from 10 to 80 to 330. It was also found that the reactor was unsuitable for tape coating on all surfaces. Hence, the design, construction and test of a new system was needed to obviate the above difficulties.

After preliminary experiments simulating the geometry of the deposition zone, a moving tape reactor was designed and constructed. Although the delivery of $NbCl_5$ was found to be desirable (Section 3), the previous $NbCl_4$ generator was retained due to the lack of time for experiments with low-temperature niobium chlorination. Use was made of furnaces, controllers, etc. employed in the previous, stationary system. All the new, additional parts were supplied and/or fabricated at Westinghouse expense.

The new, T-shaped reactor is again horizontal, due to laboratory space restrictions. All the tubing is made of vitreous silica. A schematic diagram is shown in Figure 7 and the general view of the system is shown in Figure 8. A special T-section furnace is employed to allow the vapor mixture injection from the side (T-leg) while the substrate tape runs through the straight tube (T-arms). Vapor locks and cooling chambers at each side of this straight section permit the use of external drive mechanisms. Adjustable stainless steel tracks inside the deposition zone were initially provided to allow control of the deposition zone length and position. After preliminary deposition experiments these stainless steel tracks were replaced by quartz tubes to avoid deposit contamination by steel components. Both symmetrical and asymmetrical (one side) tape

coating should be possible owing to the use of exchangeable tracks. Tape widths between 3 and 13 mm (1/8 to 1/2 in.) can be accommodated.

The motorized drive mechanism employing reels, 30 cm in diameter, is fitted with a gear mechanism ensuring the tape speed control over two orders of magnitude, from $\sim$ 30 cm/hour (1 ft) up. In preliminary experiments it was found that the drive operates satisfactorily at speeds $\geq$ 60 cm/hour. All the drive system components are mounted on carriages positioned on a track bench to permit easy reversal of the tape motion.

The electric current heating of the tape was implemented to reduce the gas phase depletion due to coating of reactor tube walls (Section 4), and thus to extend the length of the useful deposition zone. The tape was energized through carbon brush fixtures shown in Figure 3, and attached to the vapor locks at the cold ends of the reactor. The whole drive mechanism was electrically insulated from the track bench. Temperature calibration was performed for Hastelloy tape substrates 6 mm wide and 25 μm thick. Tape temperatures up to T_d = 850°C were attained for deposition zone temperatures $\geq$ 550°C.

7. References

1. G. W. Roland and A. I. Braginski, Chemical Vapor Deposition of Nb_3Ge, Adv. Cryo. Eng., 22, 347 (1977).

2. A. I. Braginski, G. W. Roland and Michael R. Daniel, Preparation of Nb_3Ge by Chemical Vapor Deposition, Appl. Polymer Symp., 29, 93 (1976).

Page Intentionally Left Blank

APPENDIX III

Presented at CEC-ICMC
Paper KA-7
Boulder, CO, August 1977

Nb_3Ge AS A POTENTIAL CANDIDATE MATERIAL FOR 15 to 25 T MAGNETS

Michael R. Daniel,* A. I. Braginski,†
G. W. Roland,* J. R. Gavaler† and A. T. Santhanam†

Westinghouse R&D Center
Pittsburgh, Pennsylvania 15235

ABSTRACT

Nb_3Ge in tape form is presently the most likely material to offer the promise of superconducting magnets in the 15 to 25 T range. The purpose of this work was to determine at 4.2 K the field dependence of critical current density, J_c (H), in fields up to 18 T parallel and perpendicular to the plane of Nb_3Ge films. The value of $J_c \simeq 1 \times 10^9$ A m^{-2}, obtained at 21 tesla for fine-grained, sputtered Nb_3Ge having a critical temperature of T_c = 22 to 23 K and an upper critical field (H_{c2}) in the range 37 to 40 T served as a target for coarse-grained Nb_3Ge samples prepared by chemical vapor deposition (CVD). In such samples the elementary fluxoid pinning was achieved by doping with a second phase such as tetragonal Nb_5Ge_3, NbN, NbC, or $NbCl_3$ in the form of fine particles dispersed in the A15 matrix. At 18 T values of J_c = 1 to 4 x 10^8 A m^{-2} could be obtained. However, the impurities responsible for effective flux pinning

---

*Work supported in part by NASA-Lewis under Contract No. NAS3-20233.

†Work supported in part by AFOSR under Contract No. F44620-70-C-0042.

also resulted in a reduction of T_c to 18 to 20 K and H_{c2} to $\leq$ 30 T. Accordingly, high field J_c values were depressed. A better trade-off between the level of flux pinning and T_c, H_{c2} degradation must be sought for Nb_3Ge grown by CVD.

Nb_3Ge AS A POTENTIAL CANDIDATE MATERIAL FOR 15 to 25 T MAGNETS

Michael R. Daniel,* A. I. Braginski,†
G. W. Roland,* J. R. Gavaler† and A. T. Santhanam†

Westinghouse R&D Center
Pittsburgh, Pennsylvania 15235

1. INTRODUCTION

The Nb_3Ge compound offers the promise as a candidate material for superconducting magnets in the 15 to 25 T range at 4.2 K. Preliminary work[1] on thin films of the sputtered material revealed this A15 superconductor possessed an upper critical field (H_{c2}) typically around 37 T at 4.2 K and a critical temperature (T_c) of 22 to 23 K. Measurements of the critical current density (J_c) gave a value of 1×10^9 A m^{-2} at 21 T, 4.2 K, the highest recorded value at this field. J_c values in the range 5×10^8 to 1×10^9 A m^{-2} at the operating field density and temperature are considered adequate for constructing a magnet. Hence, Nb_3Ge is indeed a promising material for very high field applications. Growth of Nb_3Ge by chemical vapor deposition (CVD) lends itself readily to the manufacture of lengths of conductor in tape form. The work reported on herein concentrates on the CVD material. Other fabrication techniques such as electron beam evaporation or high rate magnetron sputtering could also be amenable to the production of lengths of tape conductor.

2. TECHNIQUE

The CVD technique was a hydrogen reduction of Nb and Ge chloride vapor mixture onto 50μ thick, 1.3 and 0.6 cm wide Hastelloy B tape.[2] Reduction occurred in cylindrical tubes held at a deposition temperature between T_d = 750 and 1000°C. Deposits of Nb_3Ge* were formed on one or both sides of the Hastelloy B tape substrate and ranged in thickness from 5 to 10 μ , typically. Both short samples and up to 4 meter long tapes have been deposited.

For high-field magnet application, work concentrated on optimizing J_c through the controlled introduction of second-phase impurities into Nb_3Ge. Scanning and transmission electron microscope analysis (SEM and TEM) had revealed that single-phase (A15) Nb_3Ge deposits possess large grain structures (up to 1μ). These grain sizes were considered too large for effective fluxoid pinning and thus high J_c values. The three principal impurities or dopants concentrated upon were tetragonal Nb_5Ge_3, NbN, and NbC. At the deposition temperature of T_d = 900°C the nitrogen and carbon were introduced in gaseous form to the CVD reactor (as N_2 and C_2H_6, respectively) while the Nb_5Ge_3 could be made to occur naturally in the

---

*Nb_3Ge represents here a generic formula for the high T_c superconducting A15 phase. The actual composition of the deposit may deviate from the ideal A_3B structure.

deposit through a control of the Nb/Ge ratio in the deposition atmosphere. At deposition temperatures below T_d = 900°C Nb_5Ge_3-doping was used. In the range of T_d = 750 to 800°C the hydrogen reduction of niobium chloride, $NbCl_4$, was incomplete due to low conversion efficiency. As a result, deposited films contained occasionally a dispersed lower chloride phase, $NbCl_3$, particles of which could also serve as fluxoid pinning centers.

One immediate and important consequence of the doping was a depression of T_c to 18 to 20 K and a corresponding reduction of H_{c2}.[4] This is shown later to lead to a depression of the high field values of J_c.

The highest critical current and field values that have been reported for Nb_3Ge were measured on thin ($\sim$ 2000 Å) films that were sputtered onto sapphire or alumina substrates. To make a more direct comparison between the CVD films discussed in this paper and sputtered Nb_3Ge films, the attempt was made to sputter high-T_c Nb_3Ge onto metallic substrates. The substrates used were Hastelloy and tantalum. Although onset T_c's were obtained, in some cases, over 20 K, it was found that results were not reproducible from run to run. Also even in the best samples, transition widths were large, ΔT_c being $\sim$ 2 K or greater. Critical current and field values in these films were found to be greatly inferior to those obtained in sputtered Nb_3Ge films which were deposited on sapphire and alumina. These results therefore cannot be used to make a valid comparison between CVD and sputtered Nb_3Ge. A final conclusion to explain the difficulties thus far encountered in sputtering Nb_3Ge on metal substrates has not been reached. However it is tentatively believed

to be associated with the greater difficulty in nucleating the high-T_c phase when Nb-Ge is sputtered onto metallic substrates.

3. MEASUREMENTS

High-field J_c measurements were performed at 4.2 K by the four-point transport method on copper clad sections 3 cm long and 0.6 cm wide. Measurements were made with the magnetic field both perpendicular ($H_\perp$) and parallel ($H_{||}$) to the sample surface. Measurements of the transition temperature (T_c) and upper critical field (H_{c2}) were performed on 1.3 cm long samples using standard techniques described previously.[3,4]

4. RESULTS

Figure 1 compares TEM micrographs of Nb_3Ge films prepared by two deposition methods -- low energy sputtering and CVD. Micrograph (a) is typical of thin (< 1μ) sputtered films exhibiting high critical densities such as quoted in reference 1. Micrograph (b) shows a coarse microstructure of a 2.1μ thick CVD deposit having a low J_c. Such a material is of no practical interest. Finally micrograph (c) shows fine particles of second phase dispersed in large grains of a Nb_3Ge matrix. This microstructure is typical of CVD samples deposited at 750°C and having a J_c in excess of 1×10^8 A m^{-2} at 18 T. The second phase particle size of $\sim$ 100 Å is of the same order as the Nb_3Ge coherence length - $\xi \simeq 30$ Å at 4.2 K and should thus result in effective flux pinning. The X-ray phase analysis of such samples allows one to infer that the second phase particles are Nb_5Ge_3. Direct electron diffraction evidence could not be obtained due to the small volume fraction of particles not exceeding 5 vol. %. Samples deposited at 900°C contain particles of larger size, 300 to 600 Å, irrespective of the nature of the second phase, i.e., whether it is Nb_5Ge_3, NbN or NbC.[3] For Nb_5Ge_3 the second phase identity could be established directly by electron diffraction.[5] Of samples deposited at 900°C and characterized to date none had a J_c value as high as those deposited in the 750 to 850°C temperature range. The degree of flux pinning thus correlates with the particle size. Sections of all samples

investigated exhibit a columnar microstructure which is easily visualized by SEM.[2] The X-ray diffraction data indicates texture which becomes more pronounced with increasing film thickness. This texture is not visibly affected by the presence of second phase impurities.

Table 1 illustrates the depressant effect of an impurity dopant and of substrate on T_c and also on H_{c2} of Nb_3Ge. The data in Table 1 thus include Nb_3Ge sputtered and chemical vapor deposited on sapphire as well as Hastelloy B. The CVD samples deposited on Hastelloy are under much higher compressive stress due to thermal contraction mismatch between Nb_3Ge and the substrate. The resulting strain contributes to the depression of T_c, and H_{c2}, even in the absence of doping. Additionally a deposition on Hastelloy results in the formation of a Ni-rich diffusion layer[2] which has an adverse effect on T_c and H_{c2} especially in thinner films. Examples of high-field J_c values of CVD samples are given in Table 2 for various deposition temperatures and second-phase dopants. Figure 2 shows the high-field segment of J_c (H) curves determined for one of the representative "best" samples deposited at 750°C . In this and all other measured samples J_c ($H_\perp$) $\geq$ J_c ($H_{||}$) at all field intensities.

5. DISCUSSION

In a previous publication[6] upper limits were put on J_c for Nb_3Ge which were based on Kramer's[7] ideas of flux lattice shearing in high field and used the J_c value of 1×10^9 A m^{-2} at 21 T to fix a numerical constant. Figure 3 compares this limit with the highest J_c values so far measured for CVD Nb_3Ge (sample 277-12 contained Nb_5Ge_3 + $NbCl_3$). This plot is particularly instructive. At low fields, below 10 T, optimization of J_c through doping is clearly well advanced. The experimental curve of Figure 3 is approaching the theoretical upper limit asymptotically. However, shortcomings are evident in the high-field region where J_c is determined more by a flux shearing mechanism[7] than by flux pinning through metallurgical defects. Optimum low-field pinning has been achieved at the expense of the superconducting properties T_c and H_{c2} and thus at the expense of the high-field pinning strength. Degrading T_c to 18 K and H_{c2} to 27 T has produced a superconductor with similar properties to Nb_3Sn (T_c = 18 K, H_{c2} = 22.5 T) the dashed curve of Figure 3.

A better trade-off between T_c, H_{c2} and J_c will be necessary to suitably raise J_c for making Nb_3Ge tape for a high-field magnet. From the properties of thin sputtered films we are led to conclude a best trade-off is obtained for single-phase (A15) fine-grained deposits where flux pinning occurs predominantly on grain boundaries. This could be

achieved by CVD, for example, by drastically affecting the Nb_3Ge rate of nucleation from the gas phase or through layering. Alternatively, high-rate E-beam evaporation or magnetron sputtering could perhaps be developed to achieved fine-grained high J_c deposits.

Whichever the fabrication method used such deposits should have a nearly equiaxial, random microstructure to maximize flux pinning and to achieve $J_c(H_\perp) \simeq J_c(H_{||})$. This is of importance for superconducting solenoids since in center section the field is essentially in plane while at the coil ends it is perpendicular. Finally, a tape substrate should be sought which will minimize the strains and the diffusion of substrate components into the superconductor.

6. ACKNOWLEDGEMENTS

The high-field J_c and H_{c2} measurements were all performed at the National Magnet Laboratory (MIT) for which we acknowledge the kind hospitality of Mr. Larry Rubin. P. A. Piotrowski and H. C. Pohl provided technical assistance.

Table 1

Critical Temperature and Upper Critical Field of Nb_3Ge

Sample Designation	Deposition Temperature T_d, °C	Impurity Dopant	Transition Temperature (mid-point) T_c, K	Upper Critical Field at 4.2 K H_{c2}, T	Comments
BNGe-13 #9	750	None	22.0	37.0	Sputtered on Sapphire
A4-4B	800	None	21.5	32.5	CVD on Sapphire
201-9	900	None	21.1	31.7	CVD on Hastelloy
310-11	900	NbN	20.7	29.0	CVD on Hastelloy
201-5	900	Nb_5Ge_3	20.2	26.2	CVD on Hastelloy
279-10	750	Nb_5Ge_3	18.2	26.4	CVD on Hastelloy
335-7	900	NbC	18.2	25.2	CVD on Hastelloy

Table 2

High-Field J_c Values for Some CVD Nb_3Ge on Hastelloy

Sample Designation	Deposition Temperature T_d, °C	Dopant	Transition Temperature (mid-point) T_c, K	Nb_3Ge Thickness μ	Current Density J_c (in 10^9 A m^{-2})			
					J_c ($H_\perp$)		J_c ($H_{||}$)	
					10 T	15 T	10 T	15 T
277-12	750	Nb_5Ge_3	18.0	6.3	4.0	1.2	2.3	0.63
277-13	750	Nb_5Ge_3	18.4	6.1	3.0	0.78	1.9	0.45
229-10	800	Nb_5Ge_3	19.4	7.2	2.2	0.65	2.0	0.62
310-10	900	NbN	20.7	7.0	1.6	0.36	0.58	0.21
332-10	900	NbC	18.0	6.8	1.3	0.38	1.0	0.22

REFERENCES

* Work supported in part by NASA-Lewis under Contract No. NAS3-20233.

† Work supported in part by AFOSR under Contract No. F44620-70-C-0042.

1. Foner, S., McNiff, E. J., Jr., Gavaler, J. R. and Janocko, M. A., Phys. Lett. 47A: 485 (1975).

2. G. W. Roland and A. I. Braginski, Av. Cryo. Eng. 22: 347 (1977); A. I. Braginski, G. W. Roland and M. R. Daniel, Appl. Polymer Symp. No. 29: 43 (1976).

3. A. I. Braginski, G. W. Roland, M. R. Daniel, A. T. Santhanam and K. W. Guardipee (Westinghouse R&D Center), submitted to J. Appl. Phys.

4. A. I. Braginski, J. R. Gavaler, G. W. Roland, M. R. Daniel, M. A. Janocko and A. T. Santhanam, IEEE Trans. MAG-13: 300 (1977).

5. A. T. Santhanam (Westinghouse R&D Center), to be published in J. Appl. Phys., August 1977.

6. M. R. Daniel, Cryogenics 16: 727 (1976).

7. Edward J. Kramer, J. Appl. Phys., 44: 1360 (1973).

8. Edward J. Kramer and G. S. Knapp, J. Appl. Phys. 46: 4595 (1975).

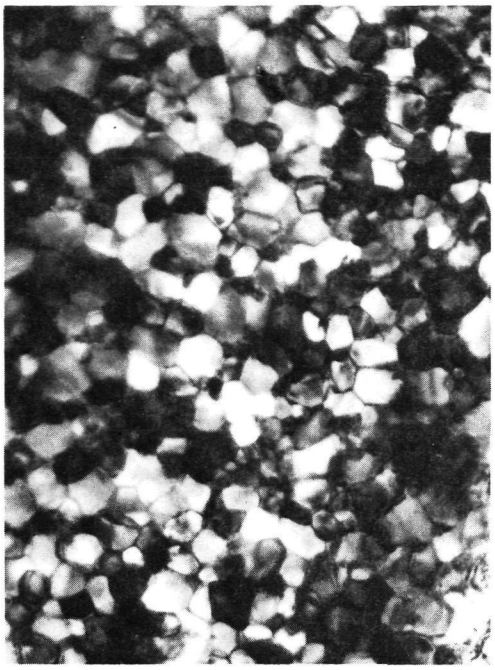

(a)

Single-phase (A15) sputtered film, average grain size 350 Å, deposition temperature 750°C.

(b)

Single-phase (A15) CVD film, average grain size 2000 Å, deposition temperature 750°C.

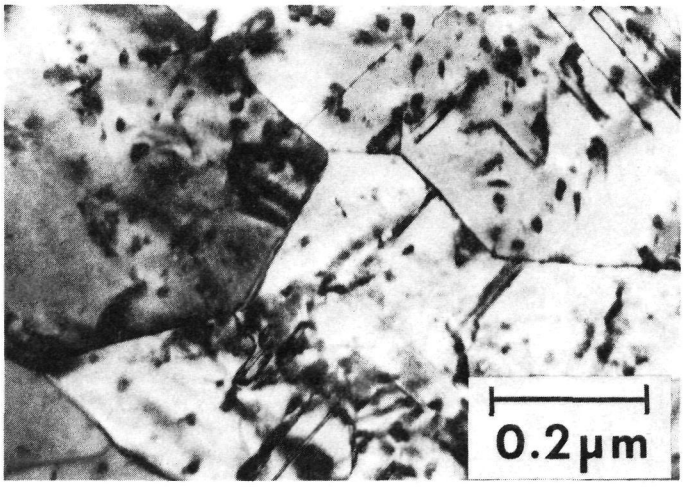

(c)

Two-phase CVD film, average grain sizes, Nb_3Ge 3000 Å, Nb_5Ge_3 50 to 200 Å, average particle spacing, 300 to 500 Å, deposition temperature 750°C.

Figure 1 - TEM micrographs of Nb_3Ge films.

Curve 691118-A

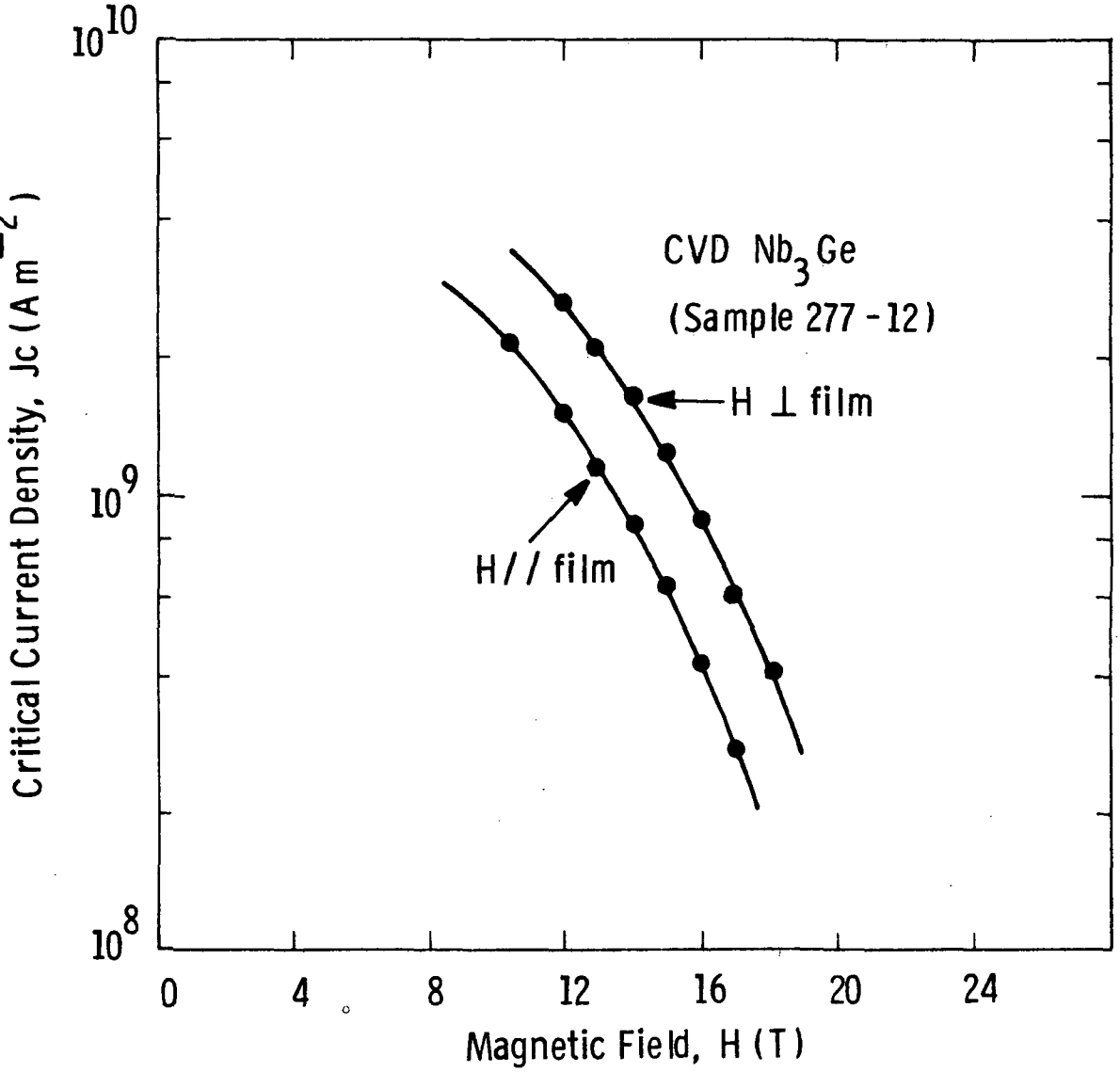

Curve 691120-A

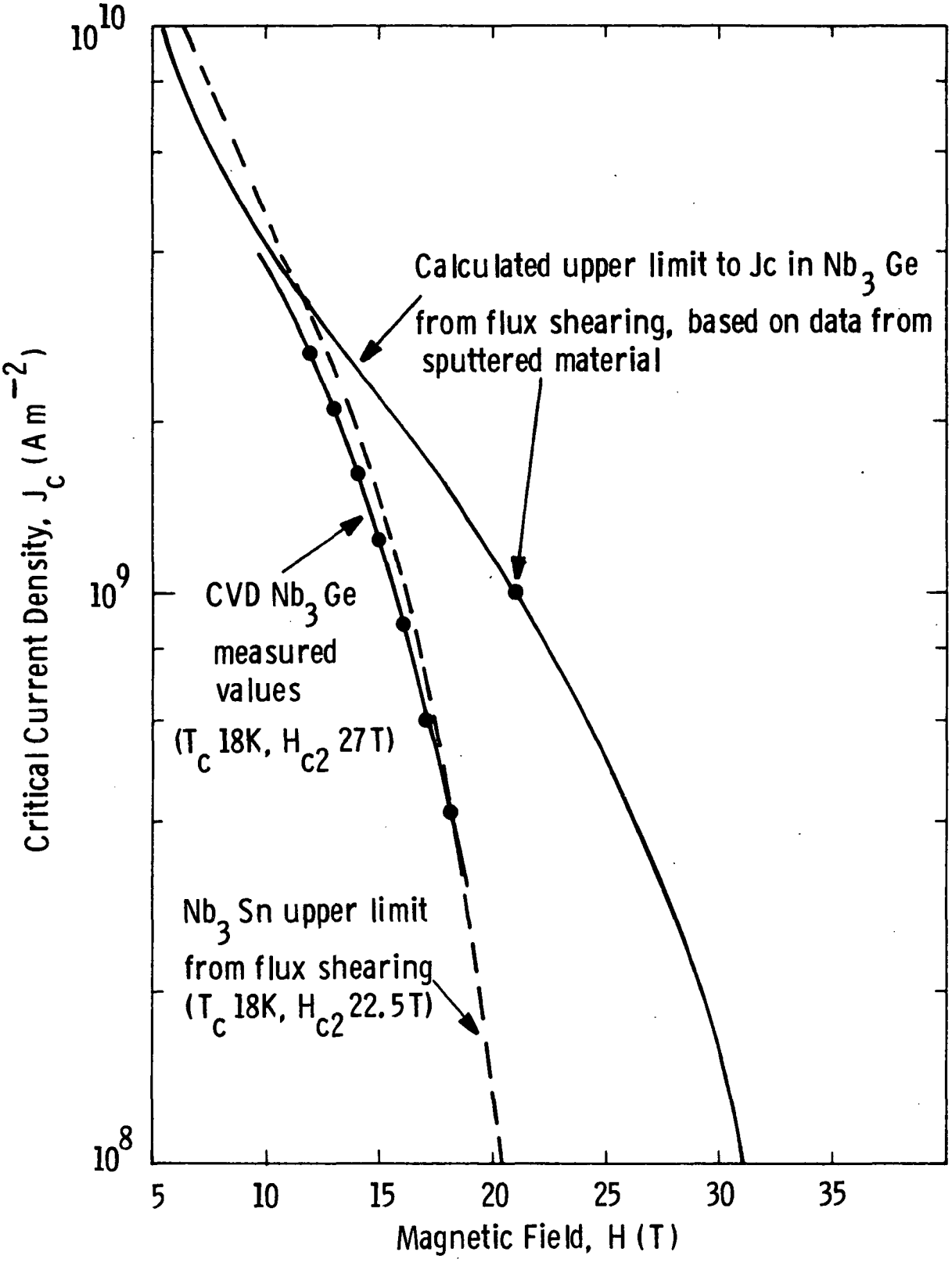

NASA DISTRIBUTION

The following distribution will be made to NASA-Lewis:

NASA-Lewis Research Center Attn: Dr. John A. Woollam, MS 301-1 21000 Brookpark Road Cleveland, Ohio 44135	3
NASA-Lewis Research Center Attn: Mr. James E. Bolander 21000 Brookpark Road Cleveland, Ohio 44135	1
NASA Scientific and Technical Information Facility Attn: Accessioning Department P. O. Box 8757 Balt./Wash. International Airport, MD 21240	30
NASA-Lewis Research Center Attn: Library (MS 60-3) 21000 Brookpark Road Cleveland, Ohio 44135	2